HHS Public Access

Author manuscript

Cell Rep. Author manuscript; available in PMC 2024 June 25.

Published in final edited form as:

Cell Rep. 2024 May 28; 43(5): 114129. doi:10.1016/j.celrep.2024.114129.

Macrophage memories of early-life injury drive neonatal nociceptive priming

Adam J. Dourson[1], **Adewale O. Fadaka**[1], **Anna M. Warshak**[1], **Aditi Paranjpe**[2], **Benjamin Weinhaus**[3], **Luis F. Queme**[1], **Megan C. Hofmann**[1], **Heather M. Evans**[4], **Omer A. Donmez**[5], **Carmy Forney**[5], **Matthew T. Weirauch**[5,6,7], **Leah C. Kottyan**[5,6,8], **Daniel Lucas**[3,8], **George S. Deepe Jr.**[9], **Michael P. Jankowski**[1,8,10,11,*]

[1]Department of Anesthesia, Division of Pain Management, Cincinnati Children's Hospital Medical Center, Cincinnati, OH, USA

[2]Biomedical Informatics, Cincinnati Children's Hospital Medical Center, Cincinnati, OH, USA

[3]Division of Experimental Hematology and Cancer Biology, Cincinnati Children's Medical Center, Cincinnati, OH, USA

[4]Division of Infectious Diseases, University of Cincinnati, Cincinnati, OH, USA

[5]Center for Autoimmune Genomics and Etiology, Cincinnati Children's Hospital Medical Center, Cincinnati, OH, USA

[6]Division of Allergy and Immunology, Cincinnati Children's Hospital Medical Center, Cincinnati, OH, USA

[7]Divisions of Biomedical Informatics and Developmental Biology, Cincinnati Children's Hospital Medical Center, Cincinnati, OH, USA

[8]Department of Pediatrics, College of Medicine, University of Cincinnati, Cincinnati, OH 45229, USA

[9]Division of Infectious Diseases, Department of Medicine, University of Cincinnati College of Medicine, Cincinnati, OH, USA

[10]Pediatric Pain Research Center, Cincinnati Children's Hospital Medical Center, Cincinnati, OH, USA

*Correspondence: michael.jankowski@cchmc.org.

AUTHOR CONTRIBUTIONS

A.J.D. and M.P.J. conceived and designed the study and wrote the manuscript. A.J.D. completed most of the experiments and collected most of the data. A.J.D. performed the analyses with input from M.P.J. A.O.F. completed the experiments at P147 and the human culture experiments. A.M.W. completed various experiments, including some IHC and qPCR. A.P. completed bioinformatics data processing. L.F.Q. assisted with *ex vivo* recordings and interpretation of data. G.S.D. and H.M.E. facilitated experiments utilizing bone marrow isolation and differentiation and stimulation of macrophages. G.S.D. helped with the conceptualization of the study. D.L. and B.W. assisted with BMT experiment planning and execution. O.A.D., C.F., M.T.W., and L.C.K. helped perform ATAC-seq and RNA-seq processing. M.C.H. managed the colony and performed genotyping assays.

SUPPLEMENTAL INFORMATION

Supplemental information can be found online at https://doi.org/10.1016/j.celrep.2024.114129.

DECLARATION OF INTERESTS

The authors declare no competing interests.

[11]Lead contact

SUMMARY

The developing peripheral nervous and immune systems are functionally distinct from those of adults. These systems are vulnerable to early-life injury, which influences outcomes related to nociception following subsequent injury later in life (i.e., “neonatal nociceptive priming”). The underpinnings of this phenomenon are unclear, although previous work indicates that macrophages are trained by inflammation and injury. Our findings show that macrophages are both necessary and partially sufficient to drive neonatal nociceptive priming, possibly due to a long-lasting remodeling in chromatin structure. The p75 neurotrophic factor receptor is an important effector in regulating neonatal nociceptive priming through modulation of the inflammatory profile of rodent and human macrophages. This “pain memory” is long lasting in females and can be transferred to a naive host to alter sex-specific pain-related behaviors. This study reveals a mechanism by which acute, neonatal post-surgical pain drives a peripheral immune-related predisposition to persistent pain following a subsequent injury.

Graphical abstract

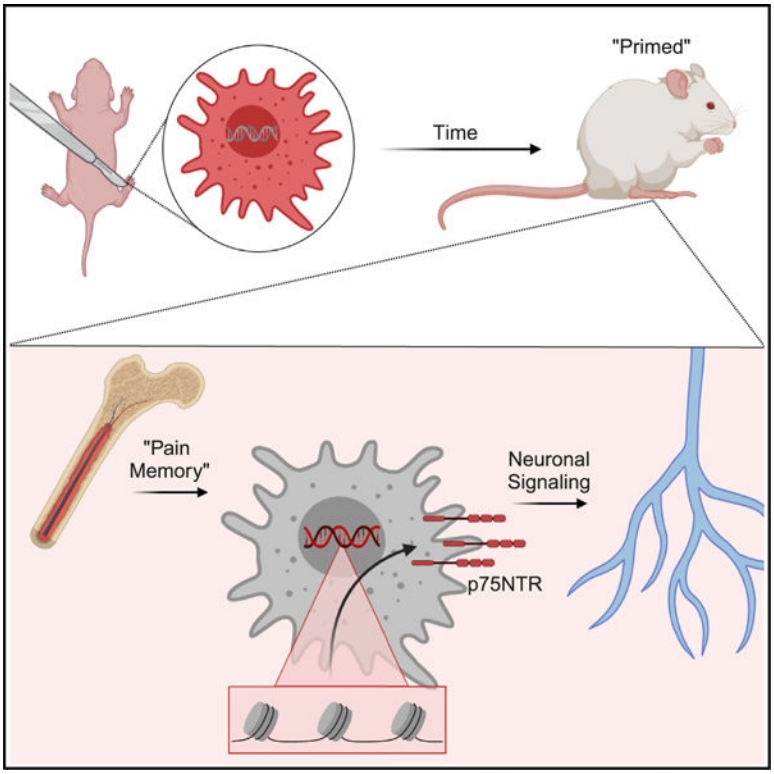

In brief

Dourson et al. investigate the effects of injury on peripheral macrophages and how they contribute to neonatal nociceptive priming. Macrophages are essential regulators of this phenomenon through modification of p75NTR. These results advance our understanding of the consequences of neonatal injury on pain processing across the lifespan.

INTRODUCTION

Peripheral injury activates several biological systems to evoke an appropriate motor and affective response to sensory stimuli. To generate and maintain nociceptive signals, there is remarkable crosstalk between cellular systems to create distinct molecular patterns that depend on the given aversive event.[1,2] Importantly, these systems undergo significant developmental changes, especially in early life,[3,4] a period when nociceptors and immune cells display unique properties compared to their adult counterparts.[5–10]

Critical periods are constrained time points of high plasticity when typical development is persistently altered by external input. Clinical studies indicate that early-life surgery or time spent in the neonatal intensive care unit alters the development of the somatosensory system.[11,12] In these patients, injury in adulthood has a higher risk of complications, including increased pain management medication use and longer hospital stays. Rodent drug studies revealed that peripheral afferent input is necessary for this phenomenon, termed "neonatal nociceptive priming."[13] However, other peripheral and developmental factors that influence this experience are unknown.

Immune cells, particularly macrophages, modulate nociceptive responses. For example, patient recovery from surgery correlates with the pre-operative inflammatory profile.[14–20] In rodents, the depletion or activation/transfer of macrophages results in differential pain-like behaviors. These studies indicate a key role for neuroimmune signaling in nociceptive responses.[5,20–23] Evidence also suggests that macrophages "learn" in response to multiple exposures of the same or similar adverse agents, likely through epigenetic remodeling characterized by changes in chromatin structure that persist following the stimulus.[24–26] While these studies indicate a cellular "memory" of these innate cells, it is unknown whether there is a similar effect after injury or whether this "memory" may affect behavior.

Aversive stimuli within the first week of life alter sensory neuron development by modifying key signaling pathways, such as neurotrophic factors.[6,7,27] Similar effects may be present in immune cells after an injury; however, much less is understood.[28,29] p75 neurotrophic factor receptor (p75NTR; also known as nerve growth factor receptor [NGFR]) modulates broad neurotrophic factor signaling pathways,[30] transcription, and the function of neurons[31] and immune cells.[28] Neurotrophins, therefore, have critical effects on the development of the nervous and immune systems and could play a dual role in both neonatal inflammation and pain.

Pediatric post-surgical pain is a major clinical health problem that is complicated by underlying differences in patients, diagnostic uncertainty, and developmental concerns.[32–35] There is often a choice between patients suffering the negative effects of pain (intensity or unpleasantness and developmental consequences) or the side effects of current treatments (non-steroidal anti-inflammatory drugs, steroids, anticonvulsants, opioids, etc.[36,37]). These and other studies clearly demonstrate that improved therapeutics designed for early-life pain are necessary for precision care.[38] Here, we aimed to investigate how early-life injury alters the peripheral neuroimmune system to "prime" animals to re-injury later in life. We

hypothesized that injury-induced epigenetic changes to chromatin accessibility in developing macrophages contribute to neonatal nociceptive priming.

RESULTS

Macrophages are necessary for neonatal nociceptive priming

Previous data indicate that macrophages are important for acute nociception in adults and neonates.[5,21,39] To establish the role of neonatal macrophages in the formation of neonatal nociceptive priming, we used macrophage fas-induced apoptosis (MaFIA) animals to ablate macrophages early in life and tested animals before and after both neonatal and adolescent incision (Figure 1A). In this animal, *Csf1r*-driven expression of FK506 binding protein 1A induces cell apoptosis when dimerized, which is temporally controlled by the injection of a designer chemical and inducer of dimerization, AP20187 (AP). Importantly, when injected, *Csf1r*+ cells undergo apoptosis, but within days of stopping the injection, new monocytes derived from the bone marrow begin to replenish lost cells.[21] We found that systemic injection of AP drastically reduced splenic macrophages but not microglia in the spinal cord (Figures S1A and S1B), similar to reports in adults.[40,41] This knockout strategy also prevented macrophage infiltration into injured muscle 1 day after a neonatal incision (Figures 1B and 1C, GFP-labeled Csf1r+ cells). Both vehicle and AP-treated groups displayed significant paw guarding 1 day after a neonatal incision, with a non-statistical decrease in AP-treated animals compared to vehicle (Figure 1D, $*p < 0.001$ vs. baseline [BL], $p = 0.071$ neonatal incision surgery [n.inc]+AP vs. n.inc+vehicle). However, while vehicle-treated animals displayed a reduction in mechanical withdrawal thresholds to muscle squeezing 1 day after incision ($*p = 0.014$ vs. BL), AP-treated animals were hyposensitive compared to BL and controls (Figure 1E, $*p = 0.007$ vs. BL, $\hat{}p = 0.028$ vs. n.inc+vehicle).

We then allowed different animals to age to post-natal day 35 (P35), when sensory neurons and immunological functions are more developed.[6,7,42,43] At this time point, we first performed evaluations to determine any long-lasting effects of early-life incision. Prior to the second incision at P35, we evaluated muscle integrity and LysM+ cell presence (Figure S1C). Evans blue dye (EBD), when administered peripherally, is unable to penetrate into myofiber bundles unless they are damaged or undergoing repair.[44] Two days post adolescent injury, we observed that about half of the myofibers were EBD positive. However, we found significantly less EBD staining within myofibers in animals that received an early-life injury or early-life sham (Figures S1D and S1E, $*p < 0.001$ vs. 2 days post incision). In addition, there were very few LysM+ cells still present in the muscle of monocyte/macrophage reporter animals (LysM;tdTom) at P35 after neonatal sham (n.sham) or n.inc surgery (Figures S1F and S1G, $p = 0.648$ vs. n.sham).

To determine the effect of early-life injury in the presence or absence of macrophages on re-injury behaviors, we evaluated MaFIA animals treated with AP or vehicle early in life that received either a P7 sham or incision surgery. After aging and prior to a second incision, we observed no differences between any groups for paw guarding or muscle squeezing. One day after the P35 incision, we confirmed that, even in neonatal AP-treated animals, muscle *Csf1r+*, GFP-expressing macrophages are present in the injured muscle (Figures 1B and 1C). At this same time, we found expected acute pain-like behaviors from

all groups. However, n.sham animals from both treatments returned to BL levels of paw guarding after day 3 (Figure 1F, *$p < 0.05$ vs. BL for all groups) and muscle withdrawal thresholds after day 7 (Figure 1G, *$p < 0.001$ vs. BL for all groups). We detected no effect of neonatal AP alone on nociceptive development in n.sham+AP animals (n.sham+vehicle vs. n.sham+AP). However, n.inc+vehicle animals displayed long-lasting pain-like behaviors after a second incision through day 14 for guarding (Figure 1F, *$p < 0.001$ vs. BL, ^$p < 0.05$ vs. n.sham+vehicle, #$p < 0.001$ vs. n.inc+AP) and day 21 for muscle squeezing (Figure 1G, *$p < 0.001$ vs. BL, ^$p < 0.005$ vs. n.sham+vehicle, #$p < 0.005$ vs. n.inc+AP). Early-life ablation of macrophages rescued this persistent pain-like phenotype, with n.inc+AP animals displaying guarding and mechanical hypersensitivity only through day 7 (Figures 1F and 1G, guarding *$p < 0.05$ vs. BL, squeezing *$p < 0.001$ vs. BL). Animals of this group were not significantly different at any time point compared to controls.

To evaluate whether the ablation of *Csf1r*+ macrophages early in life alters the sensitization of sensory neurons following dual incision, we performed intracellular recordings of individual sensory neurons in an *ex vivo* intact muscle/tibial nerve/dorsal root ganglia (DRG)/spinal cord preparation (Figure 2A). We evaluated multiple peripheral response properties 7 days after the second incision in vehicle- and AP-treated mice, where we saw a robust block of both spontaneous guarding and evoked muscle squeezing behaviors (Figures 1F and 1G). We found no difference in the conduction velocity (CV) of thinly myelinated group III afferents in animals treated with AP versus vehicle 7 days after the second incision (Figure 2B, $p = 0.987$). However, unmyelinated group IV afferents showed a significantly slower CV in AP-treated animals versus vehicle-treated animals (Figure 2C, *$p = 0.048$, example traces). After mechanical stimulation of receptive fields, we observed no change in average mechanical force necessary to evoke an action potential (Figure 2D, $p = 0.430$).

Overall, we observed no difference in the firing dynamics on all neurons collectively (Figure S2), but upon the analysis of subtypes, we found that chemosensitive and mechanically sensitive fibers (without cold responsiveness[45]) had an overall greater mechanical firing rate that was reduced following incubation with noxious metabolites (Figure 2E, *$p = 0.031$). These distinct metabolite mixtures (low or high concentration of lactic acid, protons, and ATP) activate particular neuronal subtypes associated with muscle pain.[46,47] Vehicle controls did not show a pre/post-metabolite difference. The proportion of responders in AP-treated animals resulted in a significantly higher number of responders to mechanical stimuli (42% increased to 61%) with a corresponding non-significant reduction (43% decreased to 27%) in the number of non-responder “silent” neurons (Figure 2F, *$p = 0.049$, #$p = 0.090$) compared to vehicle controls. We observed no change in the proportion of polymodal neurons (Figure S2). Finally, we found that control nociceptors displayed a direct increase in firing rate as we applied greater forces to the receptive field, as reported previously.[48] However, in animals with an early-life restricted knockout of macrophages, we found no association between firing rate and force applied (Figure 2G, *$p = 0.019$, main effect within n.inc+vehicle). We found no differences in thermal or chemical firing rate or instantaneous frequencies between groups (Figure S2). Together, these data indicate that the temporary loss of macrophages during neonatal injury changes inherent sensory neuron dynamics and decreases the ability of nociceptors to change their responsiveness over increasing mechanical forces.

Adoptive transfer of “primed” macrophages drives increased mechanical hypersensitivity

We next wanted to determine whether macrophages isolated from neonatal incised animals were sufficient to evoke a “primed” response in older mice. To do this, we performed adoptive transfer (AT) experiments in which macrophages from one animal (donor) were isolated and transferred to a sex- and age-matched naive host (Figure 3A). The *Csf1r* driver in MaFIA animals also promotes GFP expression, so we used this strain to isolate and sort peritoneal GFP+ macrophages (Figure 3B). We transferred the isolated cells into to the right hindpaw of naive hosts at P35. We first ensured that the AT was accepted by dissecting the site of injection as well as other immune-related tissues. We found GFP+ cells in wild-type hosts 3 weeks after the AT specifically at the muscle injection site and not in the nearby bone marrow, lymph node, or spleen (Figure 3C). After confirming the transfer, we found that AT of macrophages by itself (n.sham+AT alone) into an uninjured paw had no effect on paw guarding, but injection of primed cells (n.inc+AT alone) by itself induced low-level paw guarding that lasted for 1 day (Figure 3D, $*p = 0.044$ vs. BL) and slightly reduced muscle squeezing thresholds, with no difference between groups (Figure 3E, $*p < 0.05$ day 1, day 3 vs. BL). To determine how exposure to injury might evoke a differential behavioral response, we also paired the AT with a P35 incision in different animals. We found that primed cells (n.inc+AT with P35 inc), but not unprimed cells (n.sham+AT with P35 inc), when transferred into an injury environment, increased mechanical hypersensitivity compared to controls measured by muscle squeezing (Figure 3E, $^{\wedge}p < 0.01$ day 1, day 3 vs. n.sham+AT alone). This effect was not observed in paw guarding, where donor neonatal injury did not impact host behavioral outcomes, indicating a modality-directed phenotype. These data indicate that an early-life injury drives changes to macrophages that are sufficient to drive some of the enhanced behavioral phenotypes due to injury in a host environment.

Early-life incision alters the peripheral macrophage epigenetic landscape

To determine what molecular changes might be occurring in these immune cells because of early-life incision, we collected peritoneal macrophages from three different conditions of reporter animals (LysM;tdTom): naive animals with macrophages isolated at P7 (naive isolated at P7), naive macrophages isolated at P35, and P7 incised animals with macrophages isolated at P35 (P7 inc, isolated at P35 [primed]) (Figure 4A). To test whether early-life injury altered the epigenetic landscape of macrophages, we performed an assay for transposase-accessible chromatin sequencing (ATAC-seq) to measure chromatin accessibility. Quality control confirmed our isolation and predicted that the sequenced cells were macrophages (Figure S3). Principal-component analysis (PCA) revealed distinct clustering of the three groups, indicating an overall effect of early-life incision (Figure 4B). We repeated these same conditions to evaluate gene expression using RNA sequencing (RNA-seq) and found similar clustering in our bulk RNA-seq PCA (Figure 4C). We evaluated the top 100 differentially accessible chromatin sites (Figure 4D) and top 100 differentially expressed genes (DEG) (Figure 4E) from age-matched macrophages in both the P35 naive and primed groups. We obtained 10 candidate genes that were both differentially accessible and expressed in the same direction because of early-life incision (Figure 4F). From these sequencing data, we found that a promising candidate, NGFR (also known as p75NTR), was differentially regulated in macrophages due to neonatal injury (Figures 4G and 4H). p75NTR has long been of interest for nervous system development

and nociception, and it has roles in macrophage differentiation and function.[28,31] We therefore decided to test whether macrophage p75NTR could modulate neonatal nociceptive priming phenotypes.

To do this, we crossed the inducible LysMCreERT2 animal with a p75NTR floxed animal.[49] All littermates were first incised at P7 to induce priming. Beginning at P33 and continuing until P37, animals were injected with tamoxifen to eliminate p75NTR from LysM+ cells. At P35, all animals received a second incision to evoke the primed macrophage and behavioral responses. Behavior was evaluated prior to and for 3 weeks following the P35 incision (Figure 5A). To verify our injection protocol, we obtained samples following the final injection of tamoxifen at P37. We found an overall decrease of p75NTR mRNA from total peritoneal isolated cells in knockout animals compared to controls (−43% ± 51% LysMCreERT2;p75fl/fl vs. controls). A P35 incision resulted in a number of F4/80+ macrophages within the injured tissue, of which 31% were positive for p75NTR in control genotypes (Figure 5B). The knockout of p75NTR from LysM+ cells resulted in a significant reduction in co-stained (F4/80+ and p75+) macrophages (Figure 5C, $*p < 0.05$ vs. controls). Behaviorally, we observed that the knockout of p75NTR specifically in macrophages did not prevent long-lasting paw guarding (Figure 5D) but significantly blunted the severity of mechanical sensitivity 1 day following injury vs. controls (Figure 5E; $^{\wedge}p = 0.01$ vs. controls). We further determined that hypersensitivity of the contralateral paw (Figure S3, contralateral data from Figure 1) was also inhibited by p75NTR knockout in LysM+ cells (Figure S3). These data indicate that p75NTR has a partial but critical role in the macrophage-driven cellular memory that drives nociceptive priming.

Knockout of p75NTR in macrophages alters neuroimmune communication in mouse and in human induced pluripotent stem cells

We then wanted to test whether macrophage p75NTR modulated nociceptive priming through its role in inflammation in a system that could maintain a long-term immune memory. To do this, we began evaluating bone marrow-derived macrophages (BMDMs) and how they respond to neurotrophins. First, we isolated bone marrow from naive animals at P35, differentiated them into macrophages,[50] and measured cytokine release in response to different stimuli using cytokine arrays. We tested the effect of knocking down p75NTR using a small interfering RNA (siRNA) strategy (Figures 6A and S4). We tested the effect of stimulation of two neutrophins, NGF and brain-derived neurotrophic factor (BDNF), which both bind to p75NTR in addition to TrkA and TrkB, respectively. We compared these to negative (vehicle) and positive controls (lipopolysaccharide and interferon gamma [LPS+IFNγ]) controls (Figure 6B and S4). In murine cells, the knockdown of p75NTR in macrophages alone (sip75+vehicle [Veh]) affected both pro- and anti-inflammatory cytokines. If stimulated with LPS+IFNγ, then the response was predominately pro-inflammatory. NGF did not appear to alter many proteins alone in control cultures (Figure S4); however, NGF+p75NTR knockdown caused a significant downregulation of pro-inflammatory cytokine release and increased anti-inflammatory cytokine production ($*p < 0.05$ vs. siCON+Veh, $^{\wedge}p < 0.05$ vs. sip75+LPS+IFNγ, $\#p = 0.05$ vs. sip75+Veh, $\#\#p > 0.05$ vs. siP75+Veh; Figure 6C). Fewer changes were observed when BDNF or a combination of NGF and BDNF was used (Figure S4). Together with our

previous data, this may indicate that the epigenetic regulation of p75NTR in macrophages that are exposed to early-life injury could promote pro-inflammatory/pro-nociceptive factor release and that targeting this receptor can reverse this profile.

To test whether these effects are conserved in human cells to influence sensory function, we then performed similar experiments with NGF and p75NTR knockdown in human induced pluripotent stem cell (iPSC)-derived macrophages (Figure 6D). We extracted the medium of vehicle- or NGF-stimulated iPSC-derived macrophages that were treated with either control or p75-targeting siRNAs and applied it directly to human iPSC-derived sensory neurons (Figure 6E) loaded with the calcium indicator Rhodamine-2 (Rhod-2; Figure 6F). After 24-h incubation, we discovered no difference between control groups that received conditioned medium from macrophages with NGF or vehicle, but we did find a decreased calcium response to ATP in iPSC-derived sensory neurons that were previously incubated with conditioned medium from human macrophages treated with sip75+NGF (Figures 6G and 6H). No differences between groups were found after treatment with capsaicin (Figure 6I). Analyzed cells were confirmed to be viable and healthy by responding to high-KCl stimuli (Figure 6G, right). Together with our previous data, this suggests that neuroimmune signaling in murine and human cells is impacted by p75 expression.

Transplantation of neonatal “primed” bone marrow alters female incision-related behaviors

Trained immunity describes the concept of a long-lasting cellular memory that allows the immune system to display an enhanced response to subsequent insults. To determine the persistence of neonatal priming *in vivo*, we repeated the priming experiments from Figure 1. However, in these experiments, we waited 20 weeks following neonatal incision, when animals were P147, to perform the repeated hindpaw incision, followed by 3 weeks of behavioral testing. We found a persistent effect of neonatal priming in a sex-specific manner. While the effect of neonatal incision was lost in the aged males (Figures 7A and 7B), re-injured females displayed long-lasting spontaneous pain (Figure 7C, $^{\wedge}p = 0.02$ n.inc+P147 inc female vs. n.sham+P147 female at day 7) and mechanical hypersensitivity (Figure 7D, $^{\wedge}p < 0.01$ n.inc+p147 inc female vs. n.sham+P147 female at days 7 and 21) compared to neonatal females that received sham surgery.

We next hypothesized that underlying changes to bone marrow cells caused by early-life injury could be a mechanism of this retained behavioral and molecular “memory.” Therefore, we isolated mouse BMDMs at P35 from neonatal incised or sham controls. We found no difference in the total number of bone marrow cells isolated due to an incision (Figure S4). However, when we stimulated these cultured macrophages with LPS+IFNγ as an artificial second “injury” (Figure 7E), we observed that early-life injury “primed” these cells, as they responded with a greater pro-inflammatory profile compared to n.sham controls (Figure 7F, $^{*}p < 0.05$ vs. n.sham+vehicle, $^{\wedge}p < 0.05$ vs. n.sham+LPS+IFNγ [stim’d]). These results indicate that incision induces a long-lasting (at least 28 days) reprogramming of hematopoietic progenitors to generate macrophages that are primed to respond more potently to inflammation.

Finally, to test whether hematopoietic stem cells (HSCs) are a mechanism through which this long-term memory is maintained and functionally relevant to nociception, particularly

in females, we performed a bone marrow transplantation (BMT) experiment. To do this, we performed n.sham or n.inc, allowed the animals to age until P35 (where we detected an altered BMDM expression pattern), and then performed a BMT into naive adolescent mice (Figure 7G). To regain full immune functional activity following a BMT, animals recovered for 16 weeks (P147), when almost all hematopoietic cells are derived from the donated HSCs.[51,52] At this time point, animals were subjected to a hindpaw incision. We successfully transferred the bone marrow, evidenced by the vast majority of CD45.2+ donor cells and a minority of CD45.1+ host cells (Figure 7H). Prior to incision later in life, we detected an expected, but non-significant, increase in p75NTR transcript from bulk isolated peritoneal cells (128% ± 28%, one way ANOVA, n = 4–5/group). In this assay, we could not isolate macrophages specifically, so other immune cells, such as B and T cells, are contributing to these values and likely diluting the effect. Interestingly, we found that, if we analyzed female and male peritoneal cells separately, regardless of condition, females had 480% ± 25% more p75NTR than males ($p = 0.016$, ANOVA on ranks, Dunn's, n = 4–5/sex). When we evaluated all animal behavior independent of sex following later-in-life incision, we uncovered little evidence of enhanced pain-like behaviors in either group, with quick recovery in both paw guarding and muscle squeezing (Figure S5). Both groups displayed guarding behavior for only 1 day ($p < 0.001$ vs. BL) and variable mechanical hypersensitivity for 1–7 days ($p < 0.05$ vs. BL; Figure S5). However, when we separated animals by sex, although the length of injury-induced behaviors was not different between groups, and there was no acceleration or delayed onset sensitivity in males (Figures 7I and 7J), we found a delayed onset of n.sham+BMT female-specific mechanical sensitivity. However, the n.inc+BMT (primed) females displayed a leftward shift from controls (Figures 7K and 7L). One day after injury, female n.sham+BMT controls were not mechanically sensitive, but female n.inc+BMT primed-cell recipient females had significantly lower thresholds than controls ($^{\wedge}p = 0.013$ vs. controls). Together, these data describe an effect of early-life incision on HSCs that can influence evoked pain-like behaviors for over 100 days in females. Therefore, the predisposition to chronic pain due to neonatal priming is enhanced in a sex-specific manner, partially due to an HSC-related immune memory of early-life injury.

DISCUSSION

Here, we uncovered a mechanism in which the peripheral immune system can form and maintain a "pain memory" following neonatal hindpaw incision to modulate prolonged responses to repeated injury. Macrophages were found to be both necessary (Figures 1 and 2) and partially sufficient (Figure 3) to drive neonatal nociceptive priming responses at the behavioral and afferent levels. This single, local insult dramatically altered the systemic macrophage epigenetic/transcriptomic landscape (Figure 4) and function, in part through the p75NTR receptor in mouse and human cells (Figures 5 and 6). The molecular effects of early-life injury were also evident in BMDMs and following a BMT, which induced a sex-specific alteration in pain-like behavior that was functionally relevant long term in hosts (Figure 7). This study clearly demonstrates that a macrophage cellular memory formed in neonates modulates pain-related outcomes. Together, these data help us understand how

distinct cellular systems are changed by an aversive event in early development to influence nociceptive processing across the lifespan.

Previous work has evaluated vulnerable periods that exist in the somatosensory and immune systems[5,38,53–58] as well as genetic risk factors in children following surgery.[32,59] After neonatal injury, the inhibitory circuits and microglial activity of the spinal cord dorsal horn are dysregulated, leading to hyperactivity.[60–65] Moriarty et al. found that a peripheral nerve block was sufficient to prevent neonatal nociceptive priming while systemic morphine injection was not.[13] We previously demonstrated that growth hormone, which is a vital player in neonatal nociceptive development,[66] can be used to prevent neonatal nociceptive priming.[5] This highlights the importance of peripheral input to induce nociceptive priming, and our work extends these findings to include a neuroimmune mechanism.

Following an injury, there are local and global responses in the immune and nervous systems.[38] Macrophages are one of the first immune cells at the injury site to promote inflammation and subsequent wound healing. This is accomplished through damage-associated molecular patterns (DAMPs), which can be stimulated by, and control, cytokine and growth factor responses. Both DAMPs and the effector proteins released may also be pro-nociceptive, such as high-mobility group box 1, interleukin-1β, and NGF.[67–72] ATP is another DAMP that is present in our *ex vivo* preparation metabolite mixture we found to alter the mechanical firing rate of chemosensitive neurons in animals that lacked macrophages during an early-life incision (Figure 2,[68]). It may be that desensitization to a high metabolic/noxious tissue environment was a contributor to the rescue of priming by early-life macrophage ablation (Figure 1). The CV slowing of group IV sensory neurons because of macrophage ablation is an interesting result. There are reports of activity-dependent slowing of cutaneous unmyelinated fibers,[73] but this is unlikely to be the driving factor here because of the lack of spontaneous activity in these cells. There may be differences in the size of the population of neurons that could explain this phenomenon and could correlate with the differences in proportions of each type of fiber response detected (Figure 2).

AT experiments (Figure 3) showed that macrophages are only partially sufficient to induce priming. It may be that other cells, including other infiltrating or resident immune cells, “nociceptive” Schwann cells,[74] or even sensory neurons themselves, may contribute to neonatal nociceptive priming. In addition, macrophages throughout the nervous system may also play active roles in priming, such as spinal microglia.[61,64] Macrophages in the nerve and DRGs are critical regulators of nociception, and recent work has uncovered neuron-associated macrophages in the DRGs, adding the potential for direct communication between these cells, in addition to the DAMPs and signaling molecules described above.[21,39,75] However, these concepts would need further investigation.

Neonatal macrophages are unique compared to the adult, with a distinct epigenetic landscape (Figure 4) and differential responses to stimuli.[9,10,14,24,53,76] The plasticity of the macrophage epigenome is critical to differentiate monocytes to macrophages, and acute stimulation of these cells induces epigenetic modifications.[77–80] Changes in macrophages at the epigenetic level is one way in which these cells become either “trained” or “tolerant”

to subsequent stimuli.[25,26,58] Recent work by Cobo et al. reveals that infant nociceptive reflexes to noxious and non-noxious stimuli are altered by current or previous infection.[81] It is possible that an early-life aversive event, such as a surgical incision (or an infection), may generate molecular patterns that induce epigenetic priming in macrophages, as was observed here. Strategies to interrupt neuroimmune signaling may prove beneficial for these adverse injury-related effects.[82–84]

While the priming initiation mechanism is still unknown, we determined that p75NTR is one critical endpoint of the epigenetic modifications. In early development, neurotrophin signaling is necessary for sensory neuron specialization into distinct populations,[85–88] which can be modulated by p75NTR expression.[31] Macrophage p75NTR has been less studied, but HSCs express high levels of neurotrophins, and we and others found that the inflammatory response from macrophages is directly affected by a loss of p75NTR (Figure 6).[29,89,90] Developed immune cells regularly contain low levels of NTRs, but during inflammation they are robustly and transiently increased.[5,28] NGF in human derived macrophages modulates p75NTR expression and drives its co-localization with TrkA, which we found to have persistent upregulation in macrophages due to early-life incision (NCBI: GSE224209).[90] Further, Khodorova et al. demonstrated that intraplantar NGF injections evoke expected pain-like behaviors but that a general inhibition of the p75NTR receptor rescued the phenotype.[91] Combined with our data, although p75NTR was not directly assessed *ex vivo*, this indicates that immune cell p75NTR increases their pro-inflammatory signature and that ablation of this receptor can modulate pro-inflammatory signaling, blunt the ability of macrophages to communicate to sensory neurons, and partially prevent prolonged pain-like behaviors (Figures 5 and 6).

Circulating immune cells that infiltrate injury sites are constantly replenished through the bone marrow HSC pool. These are highly plastic cells that are differentially altered by injury type,[92] infection,[93] and development.[28,94] Our data support the notion that peripheral injury can alter these stem cells long term, and changes in these cells are part of a system to maintain immune-related neonatal nociceptive priming (Figures 4, 5, 6, and 7). The mechanism in which HSCs are notified of noxious stimuli is currently unknown, although there are potential avenues to be tested, including direct immune or neuronal signaling[95] or indirect signals in the blood or cerebral spinal fluid.[96] Regardless, the results we find are reminiscent of trained immunity, where an initial event is epigenetically retained in innate immune cells to enhance responses to subsequent activation.[26] In the context of immunity, the outcome is increased inflammation, while here, the outcome was enhanced nociception. Evaluation of the functional effects of injury on HSCs by BMT indicated a female-specific hastening of mechanical hypersensitivity. Interestingly, we detected no effect on spontaneous paw guarding between early-life-incised and control animals, indicating a modality-specific effect (Figure 7). It may be that “primed” macrophages have direct signaling roles that involve mechanical sensation, as we saw similar, mechanically directed effects with AT (Figure 3) and p75NTR knockout (Figure 5) behaviors. An understanding of how stem cells may be changed by peripheral injury may have important clinical considerations for a number of conditions that impact childhood development.

Limitations of the study

There are multiple technical points to consider. The depletion of macrophages in MaFIA animals alters animal activity and, in some studies, withdrawal thresholds.[39,97] In neonates, we detected no changes in BL withdrawal reflexes or guarding scores due to the knockout (Figures 1C and 1D). However, we did observe that, when we directly manipulated macrophage presence, there was an impact on withdrawal reflexes but not spontaneous behaviors (Figures 1D and 3E and our previous work[5]). Since withdrawal thresholds are some of the most utilized behavioral readouts, it may be prudent to consider multiple behavioral assays when performing experiments depleting macrophages.[5,21,39,97,98] This confound was not a major concern for adolescent/adult behaviors, however, because the animal's immune system had recovered before the second injury (Figure 1). Similar concerns are also avoided when performing AT experiments because we tested latent changes in primed macrophages, a major strength of this study.

We considered sex as a critical factor throughout our study. In our RNA-seq, we noticed some indications of differences between the sexes, especially in the early-life-incised condition. We do not have the power to critically evaluate these against one another; however, there are multiple lines of evidence that suggest that the immune-modulated injury response differs between males and females.[99] In our evaluations in aged animals, with or without a BMT, we observed female-specific impact of the early-life injury (Figure 7). Transfer of HSCs alone was not sufficient to replicate the precise timing of hypersensitivity as if the host had been injured as a neonate, but primed HSC cells did produce a leftward shift of mechanical sensitivity, again only in females. Recently, dos Santos et al. found a delayed-onset hypersensitivity in aged animals following an incision injury as well as blunted hyperalgesic priming. This was connected with changes in inflammation in older rodents compared to younger animals.[100] We found a similar delay following a BMT in female incision at P147 but not in non-BMT males or females. Nevertheless, results reveal that the relatively minor neonatal hindpaw incision injury causes "priming" of the bone marrow and resulted in a female-specific long-lasting phenotype. Indeed, when evaluating the levels of p75NTR in our BMT animals, we found that isolated female peritoneal cells had significantly more p75NTR than males. These data, along with substantial literature on the heightened prevalence of chronic pain in females,[101] warrant additional studies that examine sex differences in injury-induced changes in immune cells over time to help better understand these phenomena.

Conclusions

Clinical studies have shown that neonatal injuries have the potential to cause a "primed" somatosensory system and lead to long-term alterations in nociceptive processing.[11,12,102,103] The potential therapeutic ability of p75NTR inhibitors has been recently reviewed by Malik et al., indicating a range of functional neurological disorders that are affected by p75NTR, while Norman and McDermott review potential therapeutic strategies in blocking p75NTR signaling for pain.[104,105] New technologies that allow for the specific targeting of macrophage p75NTR could provide the specificity to prevent the priming effect on this cell type while avoiding off-target effects of the nervous system.[106] Here, we discovered a change in the epigenetic landscape of macrophages due to early-life

incision that modulated neonatal nociceptive priming. Future studies designed to analyze the immune “pain memory” may lead to important therapeutic interventions for pediatric post-surgical pain.

STAR★METHODS

RESOURCE AVAILABILITY

Lead contact—Further information and requests for resource and reagents should be directed to and will be fulfilled by the lead contact, Michael Jankowski (Michael.Jankowski@cchmc.org).

Materials availability—Materials generated in this manuscript are available upon request.

Data and code availability

- ATAC-seq and RNA-seq data are available as of the date of publication under the accession # GSE224209. Other datasets are deposited on Mendeley Data Repository: https://data.mendeley.com/datasets/xbm7kxddjt/draft?a=f13b0ef2-3721-4283-97b2-41d8e5cd2d66.
- This paper does not report original code.
- Any additional information required to reanalyze the data reported in this work paper is available from the lead contact upon request.

EXPERIMENTAL MODEL AND STUDY PARTICIPANT DETAILS

Animals—Animals of both sexes were used for all studies. Neonatal animals were considered at postnatal day 7 (P7). Adolescent animals begun experimentation at P35-P42. Adult animals were analyzed at P147. Sex was analyzed as a critical biological factor for each experiment, and differences are noted in figure legends. In an effort to reduce stress, neonatal animals were kept with the dam when not actively analyzed behaviorally, and experiments were kept as short as possible (~1 h, never more than 1.5 h). In all behavioral experiments, mice were acclimated to the room and were performed by the same experimenter under the same conditions including time of day, location, lighting and temperature. Animals were used +/− 1 day from the indicated age. All animals were kept in an environment-controlled facility at Cincinnati Children’s Hospital Medical Center with free access to food and water while on a 14/10-h light/dark cycle.

C57/Bl6 (CD45.2^{+}) mice were bred in-house or purchased from Jax (Stock#: 000664). B6.SJL/BoyJ (CD45.1^{+}) mice were bred in the CCHMC transplant core. Macrophage fas-induced apoptosis (MaFIA) animals were purchased from Jax (Stock#: 005070) and bred in-house. Myeloid/Macrophage reporter animals were generated by crossing the LysM-Cre positive animal (see Jax Stock#: 004781) with the tdTomato (tdTom) reporter mouse (B6.Cg-Gt(ROSA)26Sor$^{tm14(CAG-tdTomato)Hze}$/J) purchased from The Jackson Laboratory (Stock#: 007914). Myeloid/Macrophage specific p75NTR knockout animals were generated by crossing the tamoxifen inducible LysM-CreERT2 animal (Jax 031674) to the p75NTRfl/fl animal that was kindly donated to us by Dr. Sung Yoon at the Ohio State

University. All procedures were approved by the CCHMC Institutional Animal Care and Use Committee in compliance with AALAC approved practices.

METHOD DETAILS

Behavioral measures—Neonatal animals were transferred from their home cage to opaque chambers fitted with a translucent lid. They were acclimated for 10 min prior to any assessments. Adolescent animals were transferred from their home cage to raised chambers fitted with black side walls, translucent viewing front, back and lids, and a grid mesh bottom. These animals were acclimated for 30 min prior to any assessments. Behavioral data were gathered at neonatal baseline and one day (1d) following early life injury. Further data was gathered at adolescent baseline and 1d, 3d, 7d, 14d and 21d following adolescent injury. Behavioral assessments were performed as described before[5] and outlined below, and included a measure of spontaneous pain-like behavior as well as evoked muscle squeezing pain-like behavior.

Spontaneous pain-like behavior was measured by qualitatively assessing paw weight preference on a scale of zero to two, where zero is no guarding after injury, 1 indicates a shift in weight off of the injured paw, and 2 indicates a complete removal of the injured paw from the platform.[5] Assessments were made for a duration of 1 min every 5 min for 30 min (neonates) or 1 h (adolescents).

Muscle-directed withdrawal scores were measured using a digital pressure device (IITC Life Science Inc. Woodland Hills, CA, USA) with a dulled probe attachment ~2 mm wide at the tip. In this assay, the animal was lightly scruffed and was held upright. One at a time, the hind paws were inserted between the two arms of the device. The top arm has a flat platform to hold the dorsal hindpaw in place, while the bottom has the dulled probe. Slowly, the medial plantar paw was pressed by the probe while the animal and force were observed. When the animal gave a robust withdrawal response, the force in grams was recorded. This was repeated for a total of three trials for each animal, separated by at least 5 min between trials for recovery. The maximum squeezing force implemented to a neonate was 150 g and for an adolescent was 350 g.

Injections—To induce cell apoptosis in MaFIA animals, the designed drug AP20187 (AP; B/B Homodimerizer purchased from Takara #635058) was first prepared according to manufacturer's directions in 100% ethanol. Prior to each experiment, fresh vehicle was prepared according to manufacturer's directions for 10 mg/kg which contained 10% PEG-400, 86% Tween and 4% drug/vehicle. All animals were injected with a final volume of 30 μL by intraperitoneal (IP) injections. The drug or vehicle was added to the mixture immediately before injecting the animal. AP20187 has no known impact on wildtype (WT) animals and previous reports demonstrate that neonates injected at P1, P2, P3 and P7 show robust knockout of Csf1r expressing cells in tissue.[40,107] Tamoxifen (1000 μg at 10 mg/mL) was injected in all animals within a litter of potential LysM-CreERT2; p75NTRfl/fl genotype. The injection protocol began at P33 and was completed i.p. daily for 5 days. Animals injected with Evan's Blue Dye (EBD, Sigma E2129–10) were injected as adolescence 16–20 h prior to dissection with 200 μL of 1% EBD in sterile 0.9% saline.

Surgical hind paw incisions—Animals were anesthetized with 2–3% isoflurane. Once sufficiently anesthetized, animals were placed on their backs and their right hind paw was taped to a sterile cloth. The dorsal skin was disinfected using Chlorhaxiderm Scrub and 70% isopropyl alcohol. A longitudinal incision was made through the hairy skin lateral to the main saphenous innervation territory. The incision was continued in between the bones through to the body of the flexor digitorum brevis muscles. The muscles were then manipulated using blunt dissection techniques with #5 (neonate) and #3 (adolescent) forceps. The plantar skin was left untouched. The skin was sutured using 7–0 or 6–0 sutures for neonates and adolescents, respectively. Sham surgeries were performed exactly the same, except animals received only a suture through intact hairy hindpaw skin with no incision. Dual incision regimes were performed at both P7 and P35-P42, or P147 to the same hindpaw muscle.

Dissections—For peripheral sites, the animal was heavily anesthetized with ketamine and xylazine (100 and 16 mg/kg, respectively) and the tissue was removed. This included hind paw muscle, tibia, potineal lymph node and spleen. For neural tissue, the animal was first cardiac perfused with ice-cold saline prior to dissection where ipsilateral DRGs were removed.

Real-time PCR and protein arrays—RNA was isolated from BMDM cultures at the indicated time points using RNeasy Mini Kits (Qiagen Stock#: 74104). All isolation were performed exactly according to the manufacturer's instructions. 500ng of RNA was reverse transcribed to cDNA and real-time PCR was performed using SYBR Green Master Mix on a StepOne real-time PCR system (Applied Biosystems). Quantitative PCR was analyzed by the ΔΔcycle threshold (CT) method with normalization to GAPDH. Differences in expression and standard error are determined from the normalized ΔΔCt. This is used to calculate fold change between conditions and values are then converted to a percent change where 2-fold = 100% change.[108] Cytokines from BMDMs were analyzed using proteome profilers (R&D Systems ARY006) loaded with 700 μLs of media. One membrane was removed due to a lack of positive control expression (siCON stim LPS+IFNy). Data was first normalized to the average positive control before percent change from experimental control was calculated.

ATAC-seq and RNA-seq—Peritoneal macrophages were isolated as indicated below from P7 naive, P35 naive, and P7 incised isolated at P35 animals. Samples were pooled across two animals of the same age and sex. Samples for ATAC- and RNA-Seq were processed by the sequencing core at CCHMC. Data were analyzed by the Bioinformatics Collaborative Services at CCHMC. Briefly, shared peaks between samples were obtained by merging peaks at 50% overlap with BEDtools v2.27.0 between replicates (peaks in all biological replicates) and treatment (merge at 50% all replicate peaks). These were then converted to Gene Transfer Format and peaks were counted with feature counts v1.6.2 (Rsubread package). Raw counts were normalized as transcripts per million and peaks were annotated by the nearest or overlapping gene and genomic features using an in-house script defined by: Promoter = 1kb upstream and downstream of peak; upstream = between 21 and 1kb from peak; priority = promoter>upstream>exon>intron. The R package DESeq2 v1.26.0 was

used for differential analysis, with significance set to log2 fold change of 0.58 and FDR less than or equal to 0.05. RNA-seq was prepared similarly, where FASTQ formats were aligned to mm9 by STAR v2.6.le and stripped of duplicates by Sambamba v0.6.8. Read counts and differential expression were defined as before. Plots were generated by ggplot2 or PlotsReasy from CCHMC.

Immunohistochemistry—Freshly dissected tissue was frozen in OCT medium on dry ice or snap frozen in liquid N_2 for skeletal muscle and was then stored at −80°C. On a cryostat, tissue was sectioned at 20 μm and was melted onto a slide. Tissue was fixed in 4% paraformaldehyde, washed and blocked prior to primary antibody (WGA 1:500 (Invitrogen W32466); Dystrophin 1:250 (Abcam ab15277); p75NTR 1:1000 (Cell Signaling 82385); F4/80 1:500 (Abcam ab6640)) incubation overnight. The next day, the tissue was washed and stained with secondary antibodies before cover slipping and stained with DAPI (Fisher Scientific 17985–50.) For tissue that was genetically marked with a fluorescent dye, the tissue was post-fixed, washed, and mounted with media containing DAPI. Analysis was completed on Nikon's NIS Elements where two-three nonconsecutive sections across two-three slides were averaged to create a score for each animal. Quantification of GFP+ macrophages in Figure 1 were performed using ImageJ following similar procedures.

Macrophage isolation

Peritoneal: Animals were rapidly killed by cervical dislocation and cleaned with 70% ethanol. The peritoneum was injected with 1 mL (neonate) or 5 mLs (adolescent) of 3% fetal bovine serum (FBS) until bloated. The midsection was gently massaged to dislodge any cells, and then peritoneal fluid was extracted. Extracted peritoneal serum was processed for RNA extraction immediately, or sorted by the Flow Cytometry core at CCHMC by the LysMtdTom or MaFIA (GFP+) expression depending on the experiment and animal used. Cells were sorted in 2% FBS and into 50% FBS or PBS. Dead cells were marked with 7AAD and were removed from selection. Gating strategies were placed by the flow core and examples are presented.

Bone marrow derived macrophages (BMDM): Animals were prepared as above. The right leg was then detached from the body and placed into a dish containing HBSS. The femur and tibia were isolated, and the bone marrow was visualized by making horizontal cuts on either side of the knee. The bone marrow was flushed out of the bone with HBSS and a 22-gauge needle. HBSS with cells was collected, spun at 4°C and 1500 RPM for 5 min. The supernatant was discarded, and RPMI buffer (Catalog #11875093) supplemented with 10% fetal bovine serum (35–010-CV Lot 35010171) and gentamycin was added to resuspend the cells. GM-CSF (60 ng/mL) was added, and cells were incubated for 5 days at 37°C and 5% CO_2. Additional media and GM-CSF was added halfway through the incubation. After maturation, cells were treated with siRNAs (Origene 10 ng/uL) and stimulants (NGF, BDNF 50 ng/uL or LPS+IFNγ 10 ng/uL each) as indicated in the figure legends. Knockdown efficiency tested across three duplexes, achieved 90% by PCR. Cells were stimulated for 24 h before washing, trypsinizing, and/or scraping of the plates. Media was saved for protein array analyses. Cells were counted using a hemocytometer and then resuspended in buffer for RNA isolation using the RNeasy Mini Kit.

Adoptive transfer—Peritoneal macrophages from MaFIA animals were isolated as described above. ~80k cells were sorted into PBS. These were pelleted and reconstituted in 10 μLs of sterile PBS. Naive hosts were anesthetized and the right hindpaw was injected with all of the cells directly into either intact muscle, or the wound of a hindpaw incision before suturing. Animals were monitored following the transplant for adverse effects and behavioral responses.

Bone marrow transplant—Tibia and femur bone marrow was collected using sterile tools from adolescent animals. Under a sterile hood, bones were flushed with PBS and treated with red blood cell lysis buffer until a transparent pellet was formed after centrifugation at 1100 RMP for 4 min at 4°C. After reconstitution, cells were passed through a 70 μm filter and were counted on a hemocytometer. One million cells were transferred to a naive age and sex matched host that was previously exposed to radiation (administered in split doses, the first at 700 rads/700 cGy followed 3 h later with a second dose of 4.75 Gy (475 rads/475 cGy)) to prepare for the transplant. Animals were monitored following the transplant in their immune compromised state. We successfully completed 28 out of 32 BMTs. The animals were allowed to recover for 16 weeks prior to further experimentation, to ensure a functional immune response after transplant.[51,52]

Human induced pluripotent stem cell preparations and calcium imaging—Human induced pluripotent stem cells (iPSC) derived $CD14^+$ monocytes (ATCC, Manassas, VA, Cat No. DYS0100) were plated in macrophage differentiation medium (RPMI-1640 Medium/10% Fetal Bovine Serum (FBS), supplemented with 100 ng/mL human M-CSF, and 1% Pen/Strep) in 24 well plate at a density of 10^5 cells/ml according to manufacturer's directions. Monocytes were differentiated into macrophages within seven days. Half medium change and siRNA treatment were done at day three and day five, respectively. Briefly, 10 nM control (siCON), or siRNAs against p75NTR (sip75; Origene SR321107) were incubated with macrophages at day five in macrophage differentiation medium. At day six, macrophages treated with siRNAs were stimulated with either 50 ng/mL NGF or vehicle in macrophage differentiation medium for 24 h. At day seven, the media was extracted and used for stimulation of the sensory neurons.

Human iPSC-Derived Sensory Neuron Progenitors (AXOL; ax0555) were cultured on SureBond-XF-coated 96 well plate with Neural Plating Medium (AXOL, product codes: ax0053 and ax0033) for 24 h as recommended by the manufacturer. Briefly, full media change was achieved by replacing the neural plating medium with sensory neuron maintenance medium supplemented with growth factors (25 ng/mL Glial-Derived Neurotrophic Factor (ax139855), 25 ng/mL Nerve Growth Factor (ax139789), 10 ng/mL Brain-Derived Neurotrophic Factor (ax139800), and 10 ng/mL Neurotrophin-3 (ax139811) and sensory maturation maximizer (ax0058) at a seeding density of 50000/cm^2. Cells were treated with 2.5 μg/mL mitomycin C at day three after which the media was replaced with sensory neuron maintenance medium supplemented with growth factors and sensory maturation maximizer. Half media change was done at every three days for 21 days. All iPSC cultures and incubations were carried out in 5% CO_2/37°C.

For imaging, cells were pretreated with 5 μg/mL Rhodamine (in DMSO, ThermoFisher R1244) for 30–45 min and further dosed with equal volume of siRNA treated and stimulated macrophage media. Neuronal activities were visualized using wide-field Nikon Ti2 inverted SpectraX with 10X LWD Phase high quality objective. To analyze changes in fluorescence, regions of interest (ROIs) were randomly drawn around 15 cells across triplicate conditions. Calcium transients were measured for after stimulation with ATP (200mM) followed by capsaicin (1mM). KCl (300μM) was used as a positive control for cell viability. ΔF/FO were calculated where ΔF/FO = (Fmax – FO)/FO where Fmax: maximum intensity during stimulation and FO: the average intensity of immediately prior to stimulation.

***Ex vivo* preparation—**This preparation has recently been described in detail.[97] In this study, pups were treated with either AP or vehicle as described above and were subjected to a P7 incision followed by a P35-P42 incision. Briefly, 7d after the second incision we dissected the animal HP muscle/tibial nerve/DRG/SC in continuity in ice-cold oxygenated (95%O2/5% CO2) artificial cerebral spinal fluid (aCSF; 127.0 mM NaCl, 1.9 mM kC l, 1.2 mM KH2PO4, 1.3 mM MgSO4, 2.4 mM CaCl2, 26.0 mM NaHCO3, and 10.0 mM D-glucose: O2aCSF). The preparation was transferred to a new dish where the muscle and DRGs were isolated in separate circulating baths of O2aCSF. The temperature was slowly raised to 32°C. In L3 or L4 an electrode was filled with 5% neurobiotin and 1M potassium acetate for sharp electrode single unit recordings using Quartz electrodes (impedance>150MΩ). A suction electrode was placed on the side of the tibial nerve to send search stimuli. An impaled cell was identified by the presence of an action potential (AP) recording from the search stimulus. A receptive field on the muscle was then located using a concentric bipolar electrode. If found, the cell was counted in our analyses and mechanical, thermal and chemical stimuli were applied in that order. First von Frey fiber thresholds were identified using fibers from 0.07–10g of force applied for ~1–2 s. If the cell did not respond to the maximum, physical push was applied to determine if the cell would respond to any mechanical force. Next ice-cold saline (~2°C) was applied to the circulating bath over the receptive field, followed by hot ~53°C saline. After washout, a low concentration mixture of lactic acid, protons and ATP (applied just before stimulation) were oxygenated and flooded the muscle chamber through an in-line heater for 2 min (15 mM lactate, 1mM ATP, pH 7.0). This was repeated with a high concentration of the same metabolites (50 mM lactate, 5 mM ATP, pH 6.6). Mechanical and thermal responses were then repeated.

Activity was recorded by the Spike2 program (Cambridge Electronic Design) and was analyzed offline. At the end of the preparation the nerve length from suction electrode to DRG was measured to calculate conduction velocity (CV), where a Group IV afferent was defined as being (≤1.2 m/s) or Group III afferents (1.2–14 m/s). Mechanical thresholds were set at the minimum force required to evoke an action potential, firing rate (FR) was calculated as the maximum number events that occurred over a 200 ms bin, and instantaneous frequency (IF) was calculated to determine the maximum response to a stimulus. Distribution analyses were completed to determine if there was a shift in the number of responders in our conditions.

Statistical analyses—Data was analyzed using SigmaPlot software (v14.5). Critical significance value was set to $\alpha < 0.05$. All data were first checked for normality by Shapiro-Wilk to determine parametric or nonparametric tests. Individual tests used are described in the figure legends. Behavioral data of the same animal over time and between groups were analyzed using a two-way repeated measures (RM) ANOVA. In situations in which different animals were compared across multiple time points and groups, such as PCR data, a two-way ANOVA was used. Data at a single time points across multiple groups including much of the electrophysiological data were analyzed by a one-way ANOVA. Proportions data were analyzed using a Chi-squared or Fisher's exact test as marked in the figure legends. Graphs were made using GraphPad Prism (v9). In all experiments in which there is a potential for bias including behavior, electrophysiology, cell culture and IHC the investigator was blinded to the conditions. For behavior, animals were assigned to groups by a random number generator. Biological and technical replicates were completed for each experiment and are appropriately marked in the figure legends.

Supplementary Material

Refer to Web version on PubMed Central for supplementary material.

ACKNOWLEDGMENTS

We would like to recognize others who have provided support for this project, including The Research Flow Cytometry Core in the Division of Rheumatology and the Bio-Imaging and Analysis Facility at CCHMC; Dr. Yoon at the Ohio State University, who provided us with the p75NTRfl/fl animals; The Center for Autoimmune Genomics and Etiology (CAGE) at CCHMC; and the Comprehensive Mouse and Cancer Core for assistance with completion of the bone marrow transplantations and care for the animals. This work was supported by grants from the NIH to M.P.J. (R01NS105715 and R01NS113965), A.J.D. (F31NS122494), D.L. (R01 HL160614), and L.C.K. (P30 AR070549) and a CCHMC ARC award (53632) to L.C.K. and M.T.W. D.L. is a scholar of the Leukemia and Lymphoma Society. Cartoon schematics were created with BioRender.

REFERENCES

1. Udit S, Blake K, and Chiu IM (2022). Somatosensory and autonomic neuronal regulation of the immune response. Nat. Rev. Neurosci 23, 157–171. 10.1038/s41583-021-00555-4. [PubMed: 34997214]
2. Tamari M, Ver Heul AM, and Kim BS (2021). Immunosensation: Neuroimmune Cross Talk in the Skin. Annu. Rev. Immunol 39, 369–393. 10.1146/annurev-immunol-101719-113805. [PubMed: 33561366]
3. Karshikoff B, Tadros MA, Mackey S, and Zouikr I (2019). Neuroimmune modulation of pain across the developmental spectrum. Curr. Opin. Behav. Sci 28, 85–92. 10.1016/j.cobeha.2019.01.010. [PubMed: 32190717]
4. Spencer SJ, Galic MA, and Pittman QJ (2011). Neonatal programming of innate immune function. Am. J. Physiol. Endocrinol. Metab 300, E11–E18. 10.1152/ajpendo.00516.2010. [PubMed: 21045175]
5. Dourson AJ, Ford ZK, Green KJ, McCrossan CE, Hofmann MC, Hudgins RC, and Jankowski MP (2021). Early Life Nociception is Influenced by Peripheral Growth Hormone Signaling. J. Neurosci 41, 4410–4427. 10.1523/jneurosci.3081-20.2021. [PubMed: 33888610]
6. Fitzgerald M (2005). The development of nociceptive circuits. Nat. Rev. Neurosci 6, 507–520. 10.1038/nrn1701. [PubMed: 15995722]
7. Jankowski MP, Ross JL, Weber JD, Lee FB, Shank AT, and Hudgins RC (2014). Age-dependent sensitization of cutaneous nociceptors during developmental inflammation. Mol. Pain 10, 34. 10.1186/1744-8069-10-34. [PubMed: 24906209]

8. Jones L, Verriotis M, Cooper RJ, Laudiano-Dray MP, Rupawala M, Meek J, Fabrizi L, and Fitzgerald M (2022). Widespread nociceptive maps in the human neonatal somatosensory cortex. Elife 11, e71655. 10.7554/eLife.71655. [PubMed: 35451960]

9. Kumar SKM, and Bhat BV (2016). Distinct mechanisms of the newborn innate immunity. Immunol. Lett 173, 42–54. 10.1016/j.imlet.2016.03.009. [PubMed: 26994839]

10. Winterberg T, Vieten G, Meier T, Yu Y, Busse M, Hennig C, Hansen G, Jacobs R, Ure BM, and Kuebler JF (2015). Distinct phenotypic features of neonatal murine macrophages. Eur. J. Immunol 45, 214–224. 10.1002/eji.201444468. [PubMed: 25329762]

11. Walker SM, Melbourne A, O'Reilly H, Beckmann J, Eaton-Rosen Z, Ourselin S, and Marlow N (2018). Somatosensory function and pain in extremely preterm young adults from the UK EPICure cohort: sex-dependent differences and impact of neonatal surgery. Br. J. Anaesth 121, 623–635. 10.1016/j.bja.2018.03.035. [PubMed: 30115261]

12. Hermann C, Hohmeister J, Demirakça S, Zohsel K, and Flor H (2006). Long-term alteration of pain sensitivity in school-aged children with early pain experiences. Pain 125, 278–285. 10.1016/j.pain.2006.08.026. [PubMed: 17011707]

13. Moriarty O, Harrington L, Beggs S, and Walker SM (2018). Opioid analgesia and the somatosensory memory of neonatal surgical injury in the adult rat. Br. J. Anaesth 121, 314–324. 10.1016/j.bja.2017.11.111. [PubMed: 29935586]

14. Fragiadakis GK, Gaudillière B, Ganio EA, Aghaeepour N, Tingle M, Nolan GP, and Angst MS (2015). Patient-specific Immune States before Surgery Are Strong Correlates of Surgical Recovery. Anesthesiology 123, 1241–1255. 10.1097/aln.0000000000000887. [PubMed: 26655308]

15. Laudanski K, Zawadka M, Polosak J, Modi J, DiMeglio M, Gutsche J, Szeto WY, and Puzianowska-Kuznicka M (2018). Acquired immunological imbalance after surgery with cardiopulmonary bypass due to epigenetic over-activation of PU.1/M-CSF. J. Transl. Med 16, 143. https://www.ncbi.nlm.nih.gov/pmc/articles/PMC5970449/pdf/12967_2018_Article_1518.pdf. [PubMed: 29801457]

16. Koennecke LA, Zito MA, Proescholdt MG, van Rooijen N, and Heyes MP (1999). Depletion of systemic macrophages by liposome-encapsulated clodronate attenuates increases in brain quinolinic acid during CNS-localized and systemic immune activation. J. Neurochem 73, 770–779. [PubMed: 10428075]

17. Shutov LP, Warwick CA, Shi X, Gnanasekaran A, Shepherd AJ, Mohapatra DP, Woodruff TM, Clark JD, and Usachev YM (2016). The Complement System Component C5a Produces Thermal Hyperalgesia via Macrophage-to-Nociceptor Signaling That Requires NGF and TRPV1. J. Neurosci 36, 5055–5070. 10.1523/jneuro-sci.3249-15.2016. [PubMed: 27147658]

18. Wang YR, Mao XF, Wu HY, and Wang YX (2018). Liposome-encapsulated clodronate specifically depletes spinal microglia and reduces initial neuropathic pain. Biochem. Biophys. Res. Commun 499, 499–505. 10.1016/j.bbrc.2018.03.177. [PubMed: 29596830]

19. Mert T, Gunay I, Ocal I, Guzel AI, Inal TC, Sencar L, and Polat S (2009). Macrophage depletion delays progression of neuropathic pain in diabetic animals. Naunyn-Schmiedeberg's Arch. Pharmacol 379, 445–452. 10.1007/s00210-008-0387-3. [PubMed: 19139849]

20. Shepherd AJ, Copits BA, Mickle AD, Karlsson P, Kadunganattil S, Haroutounian S, Tadinada SM, de Kloet AD, Valtcheva MV, McIlvried LA, et al. (2018). Angiotensin II Triggers Peripheral Macrophage-to-Sensory Neuron Redox Crosstalk to Elicit Pain. J. Neurosci 38, 7032–7057. 10.1523/jneurosci.3542-17.2018. [PubMed: 29976627]

21. Shepherd AJ, Mickle AD, Golden JP, Mack MR, Halabi CM, de Kloet AD, Samineni VK, Kim BS, Krause EG, Gereau RW 4th, and Mohapatra DP (2018). Macrophage angiotensin II type 2 receptor triggers neuropathic pain. Proc. Natl. Acad. Sci. USA 115, E8057–E8066. 10.1073/pnas.1721815115. [PubMed: 30082378]

22. Pannell M, Labuz D, Celik MÖ, Keye J, Batra A, Siegmund B, and Machelska H (2016). Adoptive transfer of M2 macrophages reduces neuropathic pain via opioid peptides. J. Neuroinflammation 13, 262. 10.1186/s12974-016-0735-z. [PubMed: 27717401]

23. Jupelli M, Shimada K, Chiba N, Slepenkin A, Alsabeh R, Jones HD, Peterson E, Chen S, Arditi M, and Crother TR (2013). Chlamydia pneumoniae infection in mice induces

chronic lung inflammation, iBALT formation, and fibrosis. PLoS One 8, e77447. 10.1371/journal.pone.0077447. [PubMed: 24204830]

24. Bermick JR, Lambrecht NJ, denDekker AD, Kunkel SL, Lukacs NW, Hogaboam CM, and Schaller MA (2016). Neonatal monocytes exhibit a unique histone modification landscape. Clin. Epigenet 8, 99. 10.1186/s13148-016-0265-7.
25. Norouzitallab P, Baruah K, Biswas P, Vanrompay D, and Bossier P (2016). Probing the phenomenon of trained immunity in invertebrates during a transgenerational study, using brine shrimp Artemia as a model system. Sci. Rep 6, 21166. 10.1038/srep21166. [PubMed: 26876951]
26. Netea MG, Joosten LAB, Latz E, Mills KHG, Natoli G, Stunnenberg HG, O'Neill LAJ, and Xavier RJ (2016). Trained immunity: A program of innate immune memory in health and disease. Science 352, aaf1098. 10.1126/science.aaf1098. [PubMed: 27102489]
27. Fitzgerald M (1995). Developmental biology of inflammatory pain. Br. J. Anaesth 75, 177–185. 10.1093/bja/75.2.177. [PubMed: 7577251]
28. Bracci-Laudiero L, and De Stefano ME (2016). In Neurotoxin Modeling of Brain Disorders—Life-Long Outcomes in Behavioral Teratology, Kostrzewa RM and Archer T, eds. (Springer International Publishing), pp. 125–152.
29. Kobayashi H, and Mizisin AP (2001). Nerve growth factor and neurotrophin-3 promote chemotaxis of mouse macrophages in vitro. Neurosci. Lett 305, 157–160. 10.1016/s0304-3940(01)01854-7. [PubMed: 11403929]
30. Sajanti A, Lyne SB, Girard R, Frantzén J, Rantamäki T, Heino I, Cao Y, Diniz C, Umemori J, Li Y, et al. (2020). A comprehensive p75 neurotrophin receptor gene network and pathway analyses identifying new target genes. Sci. Rep 10, 14984. 10.1038/s41598-020-72061-z. [PubMed: 32917932]
31. Chen Z, Donnelly CR, Dominguez B, Harada Y, Lin W, Halim AS, Bengoechea TG, Pierchala BA, and Lee KF (2017). p75 Is Required for the Establishment of Postnatal Sensory Neuron Diversity by Potentiating Ret Signaling. Cell Rep 21, 707–720. 10.1016/j.cel-rep.2017.09.037. [PubMed: 29045838]
32. Dourson AJ, Willits A, Raut NGR, Kader L, Young E, Jankowski MP, and Chidambaran V (2022). Genetic and epigenetic mechanisms influencing acute to chronic postsurgical pain transitions in pediatrics: Preclinical to clinical evidence. Canadian Journal of Pain 6, 85–107. 10.1080/24740527.2021.2021799. [PubMed: 35572362]
33. Fortier MA, MacLaren JE, Martin SR, Perret-Karimi D, and Kain ZN (2009). Pediatric pain after ambulatory surgery: where's the medication? Pediatrics 124, e588–e595. 10.1542/peds.2008-3529. [PubMed: 19736260]
34. Rabbitts JA, Fisher E, Rosenbloom BN, and Palermo TM (2017). Prevalence and Predictors of Chronic Postsurgical Pain in Children: A Systematic Review and Meta-Analysis. J. Pain 18, 605–614. 10.1016/j.jpain.2017.03.007. [PubMed: 28363861]
35. Neville A, Jordan A, Pincus T, Nania C, Schulte F, Yeates KO, and Noel M (2020). Diagnostic uncertainty in pediatric chronic pain: nature, prevalence, and consequences. Pain Rep 5, e871. 10.1097/pr9.0000000000000871. [PubMed: 33251472]
36. Angst MS, Lazzeroni LC, Phillips NG, Drover DR, Tingle M, Ray A, Swan GE, and Clark JD (2012). Aversive and reinforcing opioid effects: a pharmacogenomic twin study. Anesthesiology 117, 22–37. 10.1097/ALN.0b013e31825a2a4e. [PubMed: 22713632]
37. Martin LD, Jimenez N, and Lynn AM (2017). A review of perioperative anesthesia and analgesia for infants: updates and trends to watch. F1000Res 6, 120, [version 1; referees: 2 approved]. 10.12688/f1000research.10272.1. [PubMed: 28232869]
38. Dourson AJ, and Jankowski MP (2023). Developmental impact of peripheral injury on neuroimmune signaling. Brain Behav. Immun 113, 156–165. 10.1016/j.bbi.2023.07.002. [PubMed: 37442302]
39. Yu X, Liu H, Hamel KA, Morvan MG, Yu S, Leff J, Guan Z, Braz JM, and Basbaum AI (2020). Dorsal root ganglion macrophages contribute to both the initiation and persistence of neuropathic pain. Nat. Commun 11, 264. 10.1038/s41467-019-13839-2. [PubMed: 31937758]
40. Kalymbetova TV, Selvakumar B, Rodríguez-Castillo JA, Gunjak M, Malainou C, Heindl MR, Moiseenko A, Chao CM, Vadász I, Mayer K, et al. (2018). Resident alveolar macrophages

are master regulators of arrested alveolarization in experimental bronchopulmonary dysplasia. J. Pathol 245, 153–159. 10.1002/path.5076. [PubMed: 29574785]

41. Burnett SH, Kershen EJ, Zhang J, Zeng L, Straley SC, Kaplan AM, and Cohen DA (2004). Conditional macrophage ablation in transgenic mice expressing a Fas-based suicide gene. J. Leukoc. Biol 75, 612–623. 10.1189/jlb.0903442. [PubMed: 14726498]
42. Geissmann F, Manz MG, Jung S, Sieweke MH, Merad M, and Ley K (2010). Development of monocytes, macrophages, and dendritic cells. Science 327, 656–661. 10.1126/science.1178331. [PubMed: 20133564]
43. Lissner MM, Thomas BJ, Wee K, Tong AJ, Kollmann TR, and Smale ST (2015). Age-Related Gene Expression Differences in Monocytes from Human Neonates, Young Adults, and Older Adults. PLoS One 10, e0132061. 10.1371/journal.pone.0132061. [PubMed: 26147648]
44. Millay DP, Sargent MA, Osinska H, Baines CP, Barton ER, Vuagniaux G, Sweeney HL, Robbins J, and Molkentin JD (2008). Genetic and pharmacologic inhibition of mitochondrial-dependent necrosis attenuates muscular dystrophy. Nat. Med 14, 442–447. 10.1038/nm1736. [PubMed: 18345011]
45. Jankowski MP, Rau KK, Ekmann KM, Anderson CE, and Koerber HR (2013). Comprehensive phenotyping of group III and IV muscle afferents in mouse. J. Neurophysiol 109, 2374–2381. 10.1152/jn.01067.2012. [PubMed: 23427306]
46. Light AR, Hughen RW, Zhang J, Rainier J, Liu Z, and Lee J (2008). Dorsal root ganglion neurons innervating skeletal muscle respond to physiological combinations of protons, ATP, and lactate mediated by ASIC, P2X, and TRPV1. J. Neurophysiol 100, 1184–1201. 10.1152/jn.01344.2007. [PubMed: 18509077]
47. Pollak KA, Swenson JD, Vanhaitsma TA, Hughen RW, Jo D, White AT, Light KC, Schweinhardt P, Amann M, and Light AR (2014). Exogenously applied muscle metabolites synergistically evoke sensations of muscle fatigue and pain in human subjects. Exp. Physiol 99, 368–380. 10.1113/expphysiol.2013.075812. [PubMed: 24142455]
48. Koerber HR, McIlwrath SL, Lawson JJ, Malin SA, Anderson CE, Jankowski MP, and Davis BM (2010). Cutaneous C-polymodal fibers lacking TRPV1 are sensitized to heat following inflammation, but fail to drive heat hyperalgesia in the absence of TPV1 containing C-heat fibers. Mol. Pain 6, 58. 10.1186/1744-8069-6-58. [PubMed: 20858240]
49. Follis RM, Tep C, Genaro-Mattos TC, Kim ML, Ryu JC, Morrison VE, Chan JR, Porter N, Carter BD, and Yoon SO (2021). Metabolic Control of Sensory Neuron Survival by the p75 Neurotrophin Receptor in Schwann Cells. J. Neurosci 41, 8710–8724. 10.1523/jneurosci.3243-20.2021. [PubMed: 34507952]
50. Subramanian Vignesh K, Landero Figueroa JA, Porollo A, Caruso JA, and Deepe GS Jr. (2013). Granulocyte macrophage-colony stimulating factor induced Zn sequestration enhances macrophage superoxide and limits intracellular pathogen survival. Immunity 39, 697–710. 10.1016/j.immuni.2013.09.006. [PubMed: 24138881]
51. May M, Slaughter A, and Lucas D (2018). Dynamic regulation of hematopoietic stem cells by bone marrow niches. Curr. Stem Cell Rep 4, 201–208. 10.1007/s40778-018-0132-x.
52. Ojielo CI, Cooke K, Mancuso P, Standiford TJ, Olkiewicz KM, Clouthier S, Corrion L, Ballinger MN, Toews GB, Paine R 3rd, and Moore BB (2003). Defective phagocytosis and clearance of Pseudomonas aeruginosa in the lung following bone marrow transplantation. J. Immunol 171, 4416–4424, 1950. 10.4049/jimmunol.171.8.4416. [PubMed: 14530368]
53. Spencer SJ, Martin S, Mouihate A, and Pittman QJ (2006). Early-life immune challenge: defining a critical window for effects on adult responses to immune challenge. Neuropsychopharmacology 31, 1910–1918. 10.1038/sj.npp.1301004. [PubMed: 16395304]
54. Reynolds ML, and Fitzgerald M (1995). Long-term sensory hyperinnervation following neonatal skin wounds. J. Comp. Neurol 358, 487–498. 10.1002/cne.903580403. [PubMed: 7593744]
55. Walker SM, Meredith-Middleton J, Cooke-Yarborough C, and Fitzgerald M (2003). Neonatal inflammation and primary afferent terminal plasticity in the rat dorsal horn. Pain 105, 185–195. [PubMed: 14499435]
56. Walker SM (2019). Long-term effects of neonatal pain. Semin. Fetal Neonatal Med 24, 101005. 10.1016/j.siny.2019.04.005. [PubMed: 30987942]

57. Walker SM (2019). Early life pain—effects in the adult. Current Opinion in Physiology 11, 16–24. 10.1016/j.cophys.2019.04.011.
58. Zhong XS, Winston JH, Luo X, Kline KT, Nayeem SZ, Cong Y, Savidge TC, Dashwood RH, Powell DW, and Li Q (2018). Neonatal Colonic Inflammation Epigenetically Aggravates Epithelial Inflammatory Responses to Injury in Adult Life. Cell. Mol. Gastroenterol. Hepatol 6, 65–78. 10.1016/j.jcmgh.2018.02.014. [PubMed: 29928672]
59. Chidambaran V, Zhang X, Geisler K, Stubbeman BL, Chen X, Weirauch MT, Meller J, and Ji H (2019). Enrichment of Genomic Pathways Based on Differential DNA Methylation Associated With Chronic Postsurgical Pain and Anxiety in Children: A Prospective, Pilot Study. J. Pain 20, 771–785. 10.1016/j.jpain.2018.12.008. [PubMed: 30639570]
60. Brewer CL, Li J, O'Conor K, Serafin EK, and Baccei ML (2020). Neonatal Injury Evokes Persistent Deficits in Dynorphin Inhibitory Circuits within the Adult Mouse Superficial Dorsal Horn. J. Neurosci 40, 3882–3895. 10.1523/jneurosci.0029-20.2020. [PubMed: 32291327]
61. Moriarty O, Tu Y, Sengar AS, Salter MW, Beggs S, and Walker SM (2019). Priming of Adult Incision Response by Early-Life Injury: Neonatal Microglial Inhibition Has Persistent But Sexually Dimorphic Effects in Adult Rats. J. Neurosci 39, 3081–3093. 10.1523/JNEUROSCI.1786-18.2019. [PubMed: 30796159]
62. van den Hoogen NJ, Patijn J, Tibboel D, Joosten BA, Fitzgerald M, and Kwok CHT (2018). Repeated touch and needle-prick stimulation in the neonatal period increases the baseline mechanical sensitivity and postinjury hypersensitivity of adult spinal sensory neurons. Pain 159, 1166–1175. 10.1097/j.pain.0000000000001201. [PubMed: 29528964]
63. Schwaller F, Beggs S, and Walker SM (2015). Targeting p38 Mitogen-activated Protein Kinase to Reduce the Impact of Neonatal Microglial Priming on Incision-induced Hyperalgesia in the Adult Rat. Anesthesiology 122, 1377–1390. 10.1097/aln.0000000000000659. [PubMed: 25859904]
64. Beggs S, Currie G, Salter MW, Fitzgerald M, and Walker SM (2012). Priming of adult pain responses by neonatal pain experience: maintenance by central neuroimmune activity. Brain 135, 404–417. 10.1093/brain/awr288. [PubMed: 22102650]
65. Xu Y, Moulding D, Jin W, and Beggs S (2023). Microglial phagocytosis mediates long-term restructuring of spinal GABAergic circuits following early life injury. Brain Behav. Immun 111, 127–137. 10.1016/j.bbi.2023.04.001. [PubMed: 37037363]
66. Ford ZK, Dourson AJ, Liu X, Lu P, Green KJ, Hudgins RC, and Jankowski MP (2019). Systemic growth hormone deficiency causes mechanical and thermal hypersensitivity during early postnatal development. IBRO Rep 6, 111–121. 10.1016/j.ibror.2019.02.001. [PubMed: 30815617]
67. Kato J, and Svensson CI (2015). Progress in Molecular Biology and Translational Science, Price TJ and Dussor G, eds. (Academic Press), pp. 251–279.
68. Comish PB, Carlson D, Kang R, and Tang D (2020). Damage-Associated Molecular Patterns and the Systemic Immune Consequences of Severe Thermal Injury. J. Immunol 205, 1189–1197. 10.4049/jimmunol.2000439. [PubMed: 32839211]
69. McMahon SB, Cafferty WBJ, and Marchand F (2005). Immune and glial cell factors as pain mediators and modulators. Exp. Neurol 192, 444–462. 10.1016/j.expneurol.2004.11.001. [PubMed: 15755561]
70. Basbaum AI, Bautista DM, Scherrer G, and Julius D (2009). Cellular and molecular mechanisms of pain. Cell 139, 267–284. 10.1016/j.cell.2009.09.028. [PubMed: 19837031]
71. Ren K, and Dubner R (2010). Interactions between the immune and nervous systems in pain. Nat. Med 16, 1267–1276. 10.1038/nm.2234. [PubMed: 20948535]
72. Philippou A, Maridaki M, Theos A, and Koutsilieris M (2012). Cytokines in muscle damage. Adv. Clin. Chem 58, 49–87. 10.1016/b978-0-12-394383-5.00010-2. [PubMed: 22950343]
73. Campero M, Bostock H, Baumann TK, and Ochoa JL (2011). Activity-dependent slowing properties of an unmyelinated low threshold mechanoreceptor in human hairy skin. Neurosci. Lett 493, 92–96. 10.1016/j.neulet.2011.02.012. [PubMed: 21335061]
74. Abdo H, Calvo-Enrique L, Lopez JM, Song J, Zhang MD, Usoskin D, El Manira A, Adameyko I, Hjerling-Leffler J, and Ernfors P (2019). Specialized cutaneous Schwann cells initiate pain sensation. Science 365, 695–699. 10.1126/science.aax6452. [PubMed: 31416963]

75. Guimarães RM, Aníbal-Silva CE, Davoli-Ferreira M, Gomes FIF, Mendes A, Cavallini MCM, Fonseca MM, Damasceno S, Andrade LP, Colonna M, et al. (2023). Neuron-associated macrophage proliferation in the sensory ganglia is associated with peripheral nerve injury-induced neuropathic pain involving CX3CR1 signaling. Elife 12, e78515. 10.7554/eLife.78515. [PubMed: 37254842]
76. McKelvey R, Berta T, Old E, Ji R-R, and Fitzgerald M (2015). Neuropathic Pain Is Constitutively Suppressed in Early Life by Anti-Inflammatory Neuroimmune Regulation. J. Neurosci 35, 457–466. 10.1523/jneurosci.2315-14.2015. [PubMed: 25589741]
77. Wallner S, Schröder C, Leitão E, Berulava T, Haak C, Beißer D, Rahmann S, Richter AS, Manke T, Bönisch U, et al. (2016). Epigenetic dynamics of monocyte-to-macrophage differentiation. Epigenet. Chromatin 9, 33. 10.1186/s13072-016-0079-z.
78. Foster SL, Hargreaves DC, and Medzhitov R (2007). Gene-specific control of inflammation by TLR-induced chromatin modifications. Nature 447, 972–978. 10.1038/nature05836. [PubMed: 17538624]
79. Lavin Y, Winter D, Blecher-Gonen R, David E, Keren-Shaul H, Merad M, Jung S, and Amit I (2014). Tissue-resident macrophage enhancer landscapes are shaped by the local microenvironment. Cell 159, 1312–1326. 10.1016/j.cell.2014.11.018. [PubMed: 25480296]
80. Fanucchi S, Domínguez-Andrés J, Joosten LAB, Netea MG, and Mhlanga MM (2021). The Intersection of Epigenetics and Metabolism in Trained Immunity. Immunity 54, 32–43. 10.1016/j.immuni.2020.10.011. [PubMed: 33220235]
81. Cobo MM, Green G, Andritsou F, Baxter L, Evans Fry R, Grabbe A, Gursul D, Hoskin A, Mellado GS, van der Vaart M, et al. (2022). Early life inflammation is associated with spinal cord excitability and nociceptive sensitivity in human infants. Nat. Commun 13, 3943. 10.1038/s41467-022-31505-y. [PubMed: 35803920]
82. Pinho-Ribeiro FA, Baddal B, Haarsma R, O'Seaghdha M, Yang NJ, Blake KJ, Portley M, Verri WA, Dale JB, Wessels MR, and Chiu IM (2018). Blocking Neuronal Signaling to Immune Cells Treats Streptococcal Invasive Infection. Cell 173, 1083–1097.e22. 10.1016/j.cell.2018.04.006. [PubMed: 29754819]
83. Perner C, Flayer CH, Zhu X, Aderhold PA, Dewan ZNA, Voisin T, Camire RB, Chow OA, Chiu IM, and Sokol CL (2020). Substance P Release by Sensory Neurons Triggers Dendritic Cell Migration and Initiates the Type-2 Immune Response to Allergens. Immunity 53, 1063–1077.e7. 10.1016/j.immuni.2020.10.001. [PubMed: 33098765]
84. Filtjens J, Roger A, Quatrini L, Wieduwild E, Gouilly J, Hoeffel G, Rossignol R, Daher C, Debroas G, Henri S, et al. (2021). Nociceptive sensory neurons promote CD8 T cell responses to HSV-1 infection. Nat. Commun 12, 2936. 10.1038/s41467-021-22841-6. [PubMed: 34006861]
85. Mendell LM (1996). Neurotrophins and sensory neurons: role in development, maintenance and injury. A thematic summary. Philos. Trans. R. Soc. Lond. B Biol. Sci 351, 463–467. 10.1098/rstb.1996.0043. [PubMed: 8730786]
86. Lewin GR, Ritter AM, and Mendell LM (1992). On the role of nerve growth factor in the development of myelinated nociceptors. J. Neurosci 12, 1896–1905. [PubMed: 1578276]
87. Sharma N, Flaherty K, Lezgiyeva K, Wagner DE, Klein AM, and Ginty DD (2020). The emergence of transcriptional identity in somatosensory neurons. Nature 577, 392–398. 10.1038/s41586-019-1900-1. [PubMed: 31915380]
88. Luo W, Wickramasinghe SR, Savitt JM, Griffin JW, Dawson TM, and Ginty DD (2007). A hierarchical NGF signaling cascade controls Ret-dependent and Ret-independent events during development of non-peptidergic DRG neurons. Neuron 54, 739–754. 10.1016/j.neuron.2007.04.027. [PubMed: 17553423]
89. Susaki Y, Shimizu S, Katakura K, Watanabe N, Kawamoto K, Matsumoto M, Tsudzuki M, Furusaka T, Kitamura Y, and Matsuda H (1996). Functional properties of murine macrophages promoted by nerve growth factor. Blood 88, 4630–4637. [PubMed: 8977255]
90. Williams KS, Killebrew DA, Clary GP, Seawell JA, and Meeker RB (2015). Differential regulation of macrophage phenotype by mature and pro-nerve growth factor. J. Neuroimmunol 285, 76–93. 10.1016/j.jneuroim.2015.05.016. [PubMed: 26198923]

91. Khodorova A, Nicol GD, and Strichartz G (2013). The p75NTR signaling cascade mediates mechanical hyperalgesia induced by nerve growth factor injected into the rat hind paw. Neuroscience 254, 312–323. 10.1016/j.neuroscience.2013.09.046. [PubMed: 24095693]
92. Leitão L, Alves CJ, Alencastre IS, Sousa DM, Neto E, Conceição F, Leitão C, Aguiar P, Almeida-Porada G, and Lamghari M (2019). Bone marrow cell response after injury and during early stage of regeneration is independent of the tissue-of-injury in 2 injury models. Faseb. J 33, 857–872. 10.1096/fj.201800610RR. [PubMed: 30044924]
93. Glatman Zaretsky A, Engiles JB, and Hunter CA (2014). Infection-induced changes in hematopoiesis. J. Immunol 192, 27–33, 19w50. 10.4049/jimmunol.1302061. [PubMed: 24363432]
94. Leitão L, Alves CJ, Sousa DM, Neto E, Conceição F, and Lamghari M (2019). The alliance between nerve fibers and stem cell populations in bone marrow: life partners in sickness and health. Faseb. J 33, 8697–8710. 10.1096/fj.201900454R. [PubMed: 31017803]
95. Cai R, Pan C, Ghasemigharagoz A, Todorov MI, Förstera B, Zhao S, Bhatia HS, Parra-Damas A, Mrowka L, Theodorou D, et al. (2019). Panoptic imaging of transparent mice reveals whole-body neuronal projections and skull–meninges connections. Nat. Neurosci 22, 317–327. 10.1038/s41593-018-0301-3. [PubMed: 30598527]
96. Mazzitelli JA, Smyth LCD, Cross KA, Dykstra T, Sun J, Du S, Mamuladze T, Smirnov I, Rustenhoven J, and Kipnis J (2022). Cerebrospinal fluid regulates skull bone marrow niches via direct access through dural channels. Nat. Neurosci 25, 555–560. 10.1038/s41593-022-01029-1. [PubMed: 35301477]
97. Queme LF, J Dourson A, Hofmann MC, Butterfield A, Paladini RD, and Jankowski MP (2022). Disruption of Hyaluronic Acid in Skeletal Muscle Induces Decreased Voluntary Activity via Chemosensitive Muscle Afferent Sensitization in Male Mice. eNeuro 9. 10.1523/eneuro.0522-21.2022.
98. Walker SM, Tochiki KK, and Fitzgerald M (2009). Hindpaw incision in early life increases the hyperalgesic response to repeat surgical injury: critical period and dependence on initial afferent activity. Pain 147, 99–106. 10.1016/j.pain.2009.08.017. [PubMed: 19781855]
99. Sorge RE, Mapplebeck JCS, Rosen S, Beggs S, Taves S, Alexander JK, Martin LJ, Austin JS, Sotocinal SG, Chen D, et al. (2015). Different immune cells mediate mechanical pain hypersensitivity in male and female mice. Nat. Neurosci 18, 1081–1083. 10.1038/nn.4053. [PubMed: 26120961]
100. dos Santos NL, Lenert ME, Castillo ZW, Mody PH, Thompson LT, and Burton MD (2023). Age and Sex Drive Differential Behavioral and Neuroimmune Phenotypes During Postoperative Pain. Neurobiol. Aging 123, 129–144. 10.1016/j.neurobiolaging.2022.09.008. [PubMed: 36577640]
101. Mogil JS (2020). Qualitative sex differences in pain processing: emerging evidence of a biased literature. Nat. Rev. Neurosci 21, 353–365. 10.1038/s41583-020-0310-6. [PubMed: 32440016]
102. Peters JWB, Schouw R, Anand KJS, van Dijk M, Duivenvoorden HJ, and Tibboel D (2005). Does neonatal surgery lead to increased pain sensitivity in later childhood? Pain 114, 444–454. 10.1016/j.pain.2005.01.014. [PubMed: 15777869]
103. Williams MD, and Lascelles BDX (2020). Early Neonatal Pain-A Review of Clinical and Experimental Implications on Painful Conditions Later in Life. Front. Pediatr 8, 30. 10.3389/fped.2020.00030. [PubMed: 32117835]
104. Malik SC, Sozmen EG, Baeza-Raja B, Le Moan N, Akassoglou K, and Schachtrup C (2021). In vivo functions of p75(NTR): challenges and opportunities for an emerging therapeutic target. Trends Pharmacol. Sci 42, 772–788. 10.1016/j.tips.2021.06.006. [PubMed: 34334250]
105. Norman BH, and McDermott JS (2017). Targeting the Nerve Growth Factor (NGF) Pathway in Drug Discovery. Potential Applications to New Therapies for Chronic Pain. J. Med. Chem 60, 66–88. 10.1021/acs.jmedchem.6b00964. [PubMed: 27779399]
106. Zhao Z, Ukidve A, Kim J, and Mitragotri S (2020). Targeting Strategies for Tissue-Specific Drug Delivery. Cell 181, 151–167. 10.1016/j.cell.2020.02.001. [PubMed: 32243788]
107. Burnett SH, Beus BJ, Avdiushko R, Qualls J, Kaplan AM, and Cohen DA (2006). Development of peritoneal adhesions in macrophage depleted mice. J. Surg. Res 131, 296–301. 10.1016/j.jss.2005.08.026. [PubMed: 16289593]

108. Queme LF, Weyler AA, Cohen ER, Hudgins RC, and Jankowski MP (2020). A dual role for peripheral GDNF signaling in nociception and cardiovascular reflexes in the mouse. Proc. Natl. Acad. Sci. USA 117, 698–707. 10.1073/pnas.1910905116. [PubMed: 31848242]

Highlights

- Macrophages are trained by injury and drive neonatal nociceptive priming
- Enrichment of p75NTR in macrophages alters neuroimmune signaling
- Injury-encoded cellular memories may be maintained by bone marrow stem cells

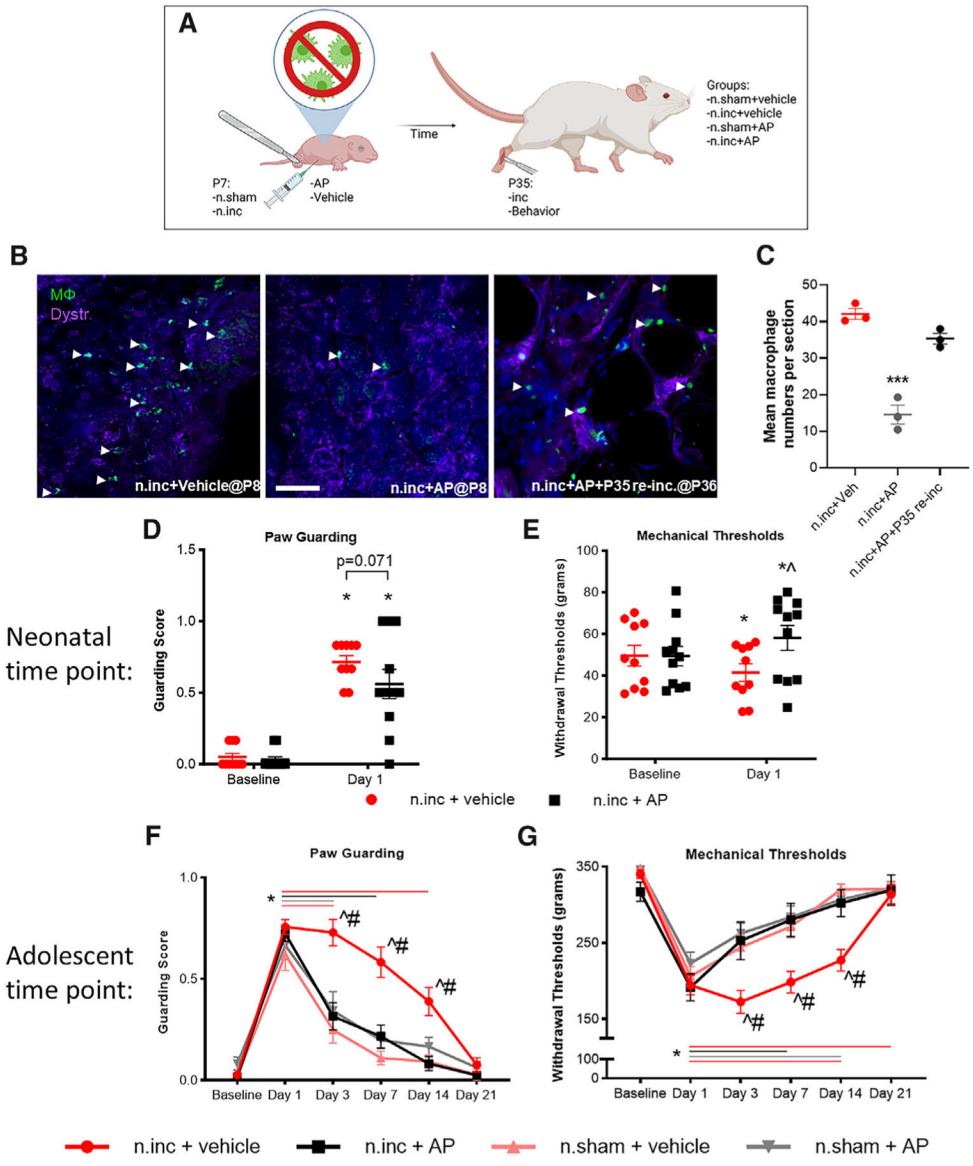

Figure 1. Early-life ablation of macrophages alters responses to re-injury later in life

(A) Schematic of the experimental design used in MaFIA mice.

(B and C) Treatment of MaFIA animals with AP early in life was sufficient to ablate macrophages (Csf1r+ cells, GFP) at the injury site 1 day after neonatal incision. Macrophages are present in the hindpaw of a P35 injured animal even after neonatal AP treatment (***$p < 0.001$ vs. n.inc+vehicle and n.inc+ AP+P35 re-inc.; one-way ANOVA, Tukey's; $n = 3$ per group). Scale bar, 25 μM.

(D) Paw guarding 1 day after neonatal incision with or without macrophage ablation indicated an effect of day (F = 103.418) but no difference between groups (*$p < 0.001$ vs. BL for AP- and vehicle-treated animals; $p = 0.071$ AP treated vs. vehicle treated).

(E) Muscle squeezing showed an interaction for withdrawal thresholds (F = 16.647). Vehicle-treated animals had a significant reduction from baseline (BL) (*$p = 0.014$ vs. BL), while incision+AP animals were hyposensitive and different from controls (*$p = 0.007$ vs.

BL; groups were $^{\wedge}p = 0.028$ vs. controls; two-way repeated measures (RMs) ANOVA; $n =$ 10–11/group).

(F) Animals that received early-life ablation of macrophages (n.inc+AP) did not have altered BL scores at adolescence, but the response to a second injury revealed a significant effect of dual incision (guarding F = 5.635, muscle squeezing F = 5.303). Groups that received a sham as neonates (n.sham+vehicle, n.sham+AP) guarded through day 3 ($*p < 0.01$ vs. BL), while vehicle-treated dually incised animals guarded through day 14 ($*p < 0.001$ vs. BL). Animals from the neonatal incision (n.inc+AP) group returned to BL guarding scores after 7 days ($*p < 0.05$ vs. BL). At days 3, 7, and 14, the n.inc+vehicle group was significantly different compared to all other groups ($^{\wedge}p < 0.05$ n.inc+vehicle vs. controls, $\#p < 0.001$ vs. n.inc+AP).

(G) For muscle squeezing withdrawal thresholds, n.sham-operated groups were hypersensitive through day 7 ($*p < 0.005$ vs. BL). The n.inc+vehicle group showed reduced thresholds through day 14 ($*p < 0.001$ vs. BL), but n.inc+AP-treated animals were hypersensitive only through day 3 ($*p < 0.001$ vs. BL). At days 3, 7 and 14, the n.inc+vehicle group had significantly lower thresholds compared to all other groups ($^{\wedge}p <$ 0.005 vs. controls, $\#p < 0.005$ vs. n.inc+AP). Colored horizontal lines indicate duration of significance compared to BL for each group. Mean ± SEM.

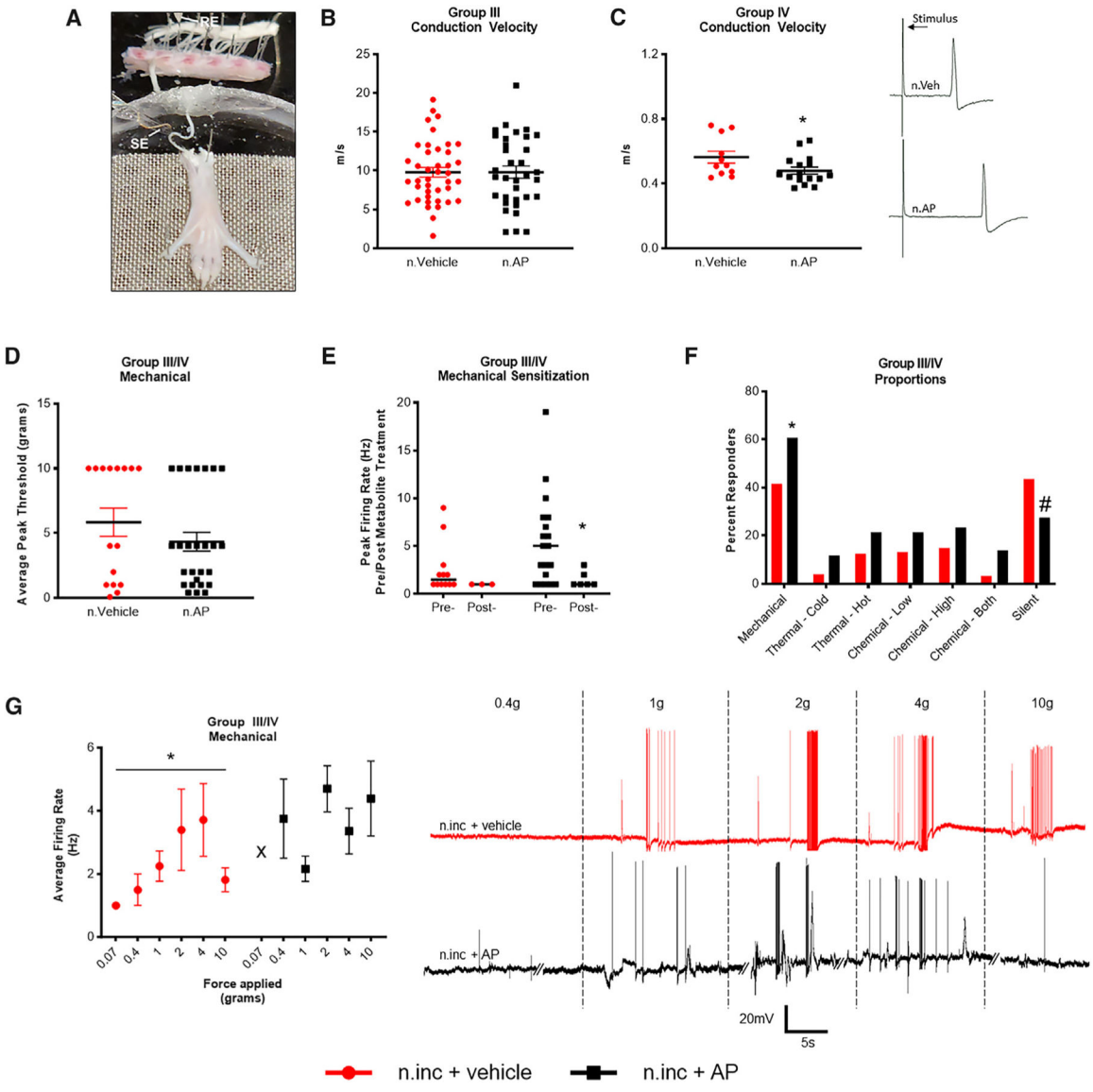

Figure 2. Macrophage depletion in neonates alters sensory neuron sensitization following repeated incision

(A) Representative image of the hindpaw muscle electrophysiological preparation. SE, suction electrode; RE, recording electrode.

(B and C) No difference in CVs in group III muscle afferents were found (B) ($p = 0.987$ n.inc+AP vs. n.inc+vehicle; $n = 34$ and 39, respectively; one-way ANOVA, Tukey's), but (C) there was a significant reduction of group IV CVs (H = 3.896) in neonatally treated AP group vs. vehicle (*$p = 0.048$ n.inc+AP vs. n.inc+vehicle; $n = 16$ and 11, respectively; ANOVA on ranks, Dunn's). Shown are example traces of action potential dynamics evoked within each group. The electrical stimulus artifact precedes the evoked action potential.

(D) There are no differences in mechanical thresholds between groups ($p = 0.430$ n.inc+AP vs. n.inc+vehicle; $n = 31$ and 22, respectively; ANOVA on ranks, Dunn's).

(E) There is no change in mechanical firing rate pre to post metabolite treatment in vehicle-treated mice, unlike that seen in AP-treated mice (H = 4.934, n.inc+ vehicle: $p = 0.223$, n.inc+AP: $*p = 0.031$, ANOVA on ranks, Dunn's).
(F) There is an increase in the number of mechanically sensitive cells in AP-treated animals vs. vehicle ($*p = 0.049$ n.inc+AP vs. n.inc+vehicle, chi-square), with a corresponding non-significant decrease in cells that responded to no stimulus ("silent," $\#p = 0.090$ n.inc+AP vs. n.inc+vehicle, chi-square on silent neurons).
(G) There is a significant increase in firing rate over mechanical forces in the vehicle treatment (H = 5.760) but not in the AP treatment group (n.inc+vehicle: $*p = 0.019$, one way ANOVA on ranks, Dunn's; n.inc+AP: $p = 0.149$, one-way ANOVA on ranks, Dunn's; "X" = no cell responded to that force). Shown are example traces of a single cell per group, indicating the response to subsequent increasing forces applied to the cell's receptive field. Mean ± SEM.

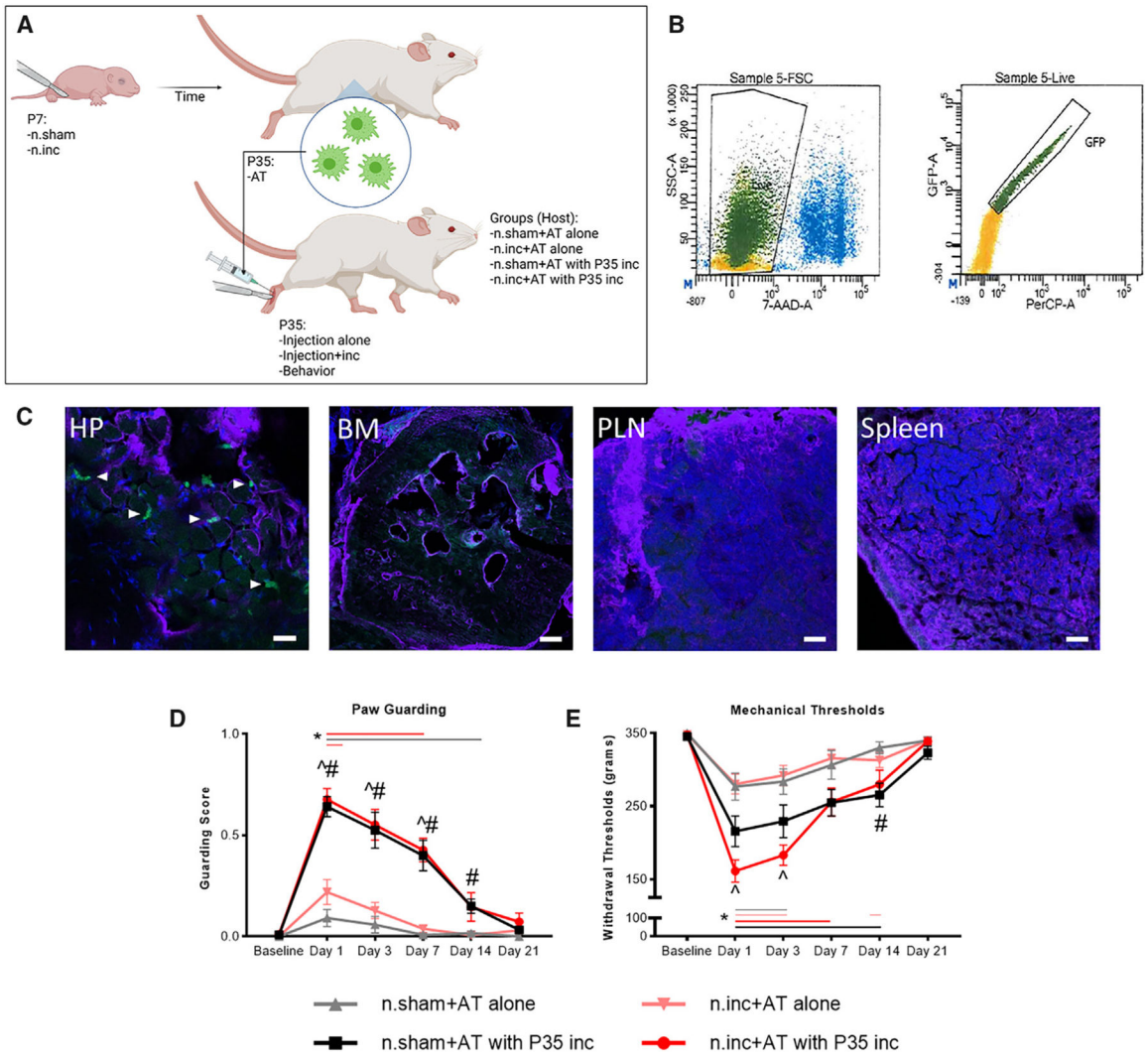

Figure 3. AT of macrophages from neonatal incised animals increases pain-like behaviors

(A) Experimental design.

(B) Example of live sorting of GFP+ peritoneal macrophages from MaFIA mice.

(C) Example images demonstrating the presence of GFP+ donated cells (arrows) in the hindpaw of a host 21 days after injection but not in the bone marrow (ipsilateral tibia), lymph node (potineal), or spleen. Scale bars, 25 μM; BM, 150 μM.

(D) For guarding, there was an effect ($F = 3.132$) of macrophage exposure to injury. Both primed (n.inc+AT with P35 inc) and unprimed (n.sham+AT with P35 inc) cells injected into an incision site induced prolonged guarding ($*p < 0.05$ vs. BL). In the absence of injury at P35, primed (n.inc+AT alone) cells induced 1 day of guarding ($*p = 0.044$ vs. BL) while unprimed cells (n.sham+AT alone) did not. There was a significant difference between n.inc+AT with P35 inc and n.sham+AT alone at days 1, 3, and 7 ($\hat{}p < 0.001$ vs. n.sham+AT alone) and between n.sham+AT with P35 inc vs. n.sham+AT alone at days 1–14 ($\#p < 0.05$ vs. n.sham).

(E) For muscle squeezing withdrawal thresholds, there was a significant interaction ($F = 4.318$). All groups had a significant reduction in withdrawal thresholds that varied

over time depending on condition (*$p < 0.05$ vs. BL). N.inc+AT with P35 incision was significantly different than n.sham+AT alone at days 1 and 3 ($^{\wedge}p < 0.01$ vs. n.sham+AT alone). N.sham+AT with P35 incision vs. n.sham+AT alone treatment showed an effect at day 14 (#$p = 0.015$ vs. n.sham+AT alone). Two-way RM ANOVA, Tukey's post hoc, n = 8–11/group. Colored horizontal lines indicate duration of significance compared to BL for each group. Mean ± SEM.

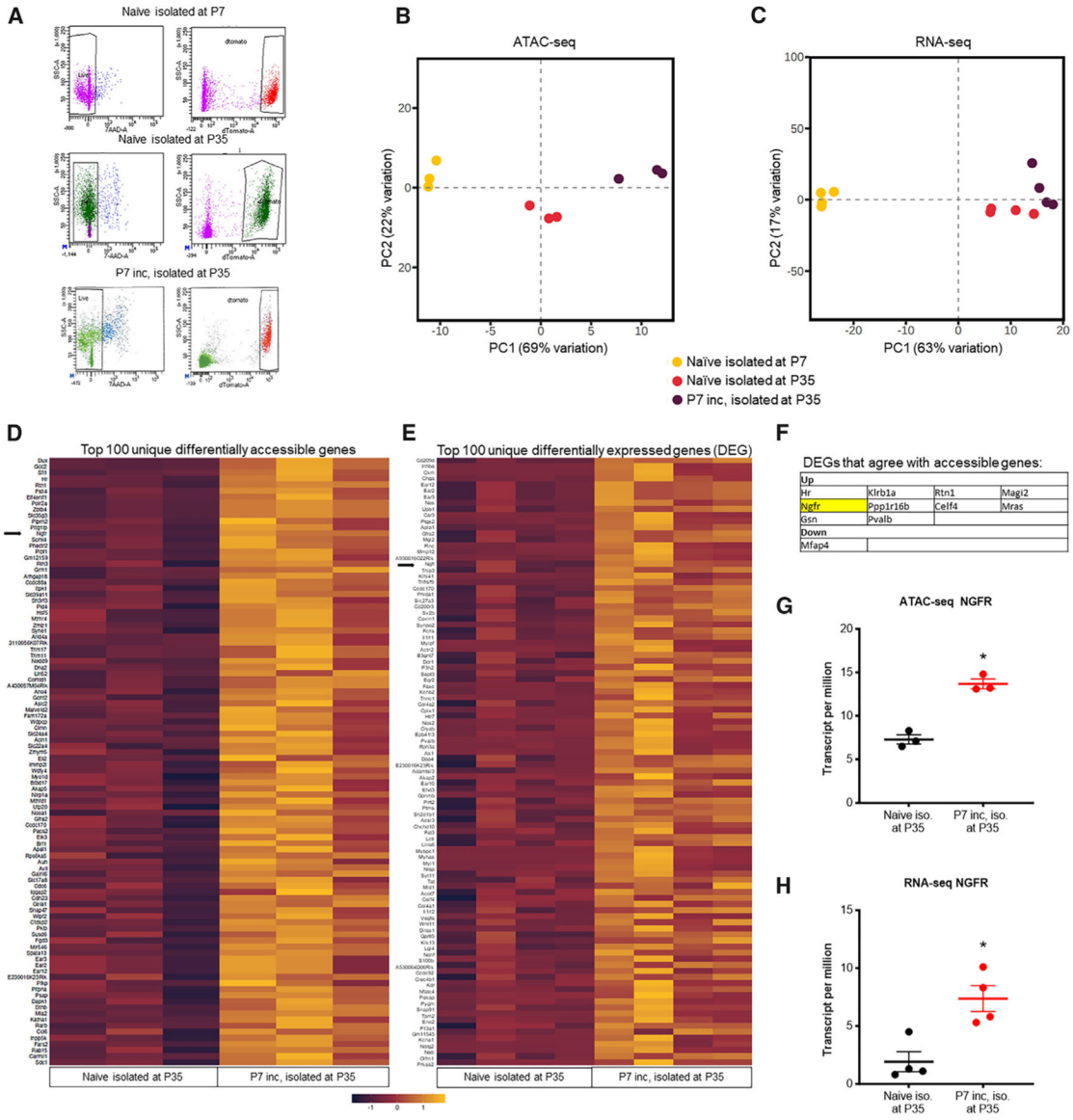

Figure 4. Early-life incision alters the epigenetic and mRNA landscape of LysM+ cells

(A) Example sorting of peritoneal macrophages from indicated conditions.

(B) PCA from ATAC-seq datasets.

(C) PCA form the RNA-seq dataset.

(D) The top 100 differentially accessible chromatin regions in macrophages in P35 naive cells compared to P35 primed cells (age matched).

(E) The top 100 differentially expressed genes (DEGs) for the same conditions.

(F) A table of factors that had differentially accessible regions and DEGs. NGFR (p75NTR) is indicated.

(G and H) ATAC-seq (G) indicating higher reads of NGFR (*p = 0.001 vs. controls, one-way ANOVA, Tukey's, n = 3–4/group) and (H) transcripts per million data for RNA-seq (*p = 0.008 vs. controls). Mean ± SEM.

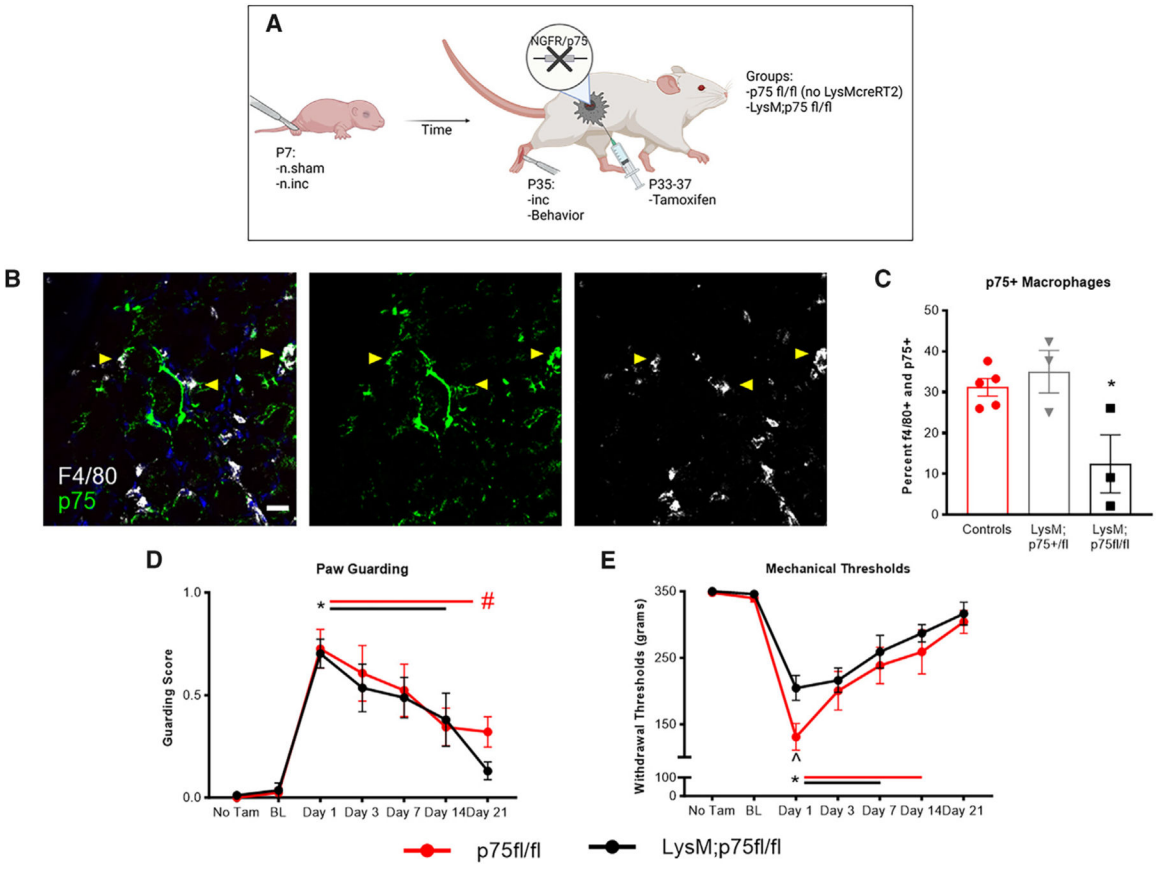

Figure 5. Macrophage-specific knockout of p75NTR after neonatal incision impacts neonatal nociceptive priming

(A) Schematic of knocking out p75NTR from macrophages following neonatal incision.

(B) Representative images of p75NTR labeling (green) co-stained with F4/80 (macrophages, white) in the injured hindpaw. Yellow arrows, double-positive staining. Scale bar, 25 μM.

(C) There is a significant reduction ($F = 4.012$) in the percentage of double-positive cells in LysM;p75fl/fl animals compared to other genotypes (*$p < 0.05$ vs. controls (p75+/fl and p75 fl/fl) and LysM; p75+/fl, one way ANOVA, Tukey's, n = 3–5/group).

(D) We found no effect of tamoxifen prior to the second injury (No Tam vs. BL time points) on paw guarding. Following the second incision, there was robust paw guarding ($F = 26.258$) with a faster recovery in the LysM;p75NTRfl/fl mice (*$p < 0.05$ vs. BL, #$p = 0.05$ vs. BL p75 fl/fl, two-way RM ANOVA, Tukey's).

(E) No effect of tamoxifen on mechanical withdrawal thresholds was found prior to injury (No Tam vs. BL time points); however, there was an effect following a second incision ($F = 40.516$). Both groups displayed mechanical sensitivity on days 1, 3, and 7 (*$p < 0.01$ vs. BL). p75fl/fl controls continued to display significant sensitivities at day 14 while LysM; p75 fl/fl animals did not (p75fl/fl: *$p = 0.002$ vs. BL, LysM;p75fl/fl: $p = 0.063$ vs. BL). One day following the second incision, LysM;p75fl/fl animals were less hypersensitive than controls ($^{\wedge}p = 0.01$ vs. controls). Two-way RM ANOVA, Tukey's, $n = 7$/group. Colored horizontal lines indicate the duration of significance compared to BL for each group. Mean ± SEM.

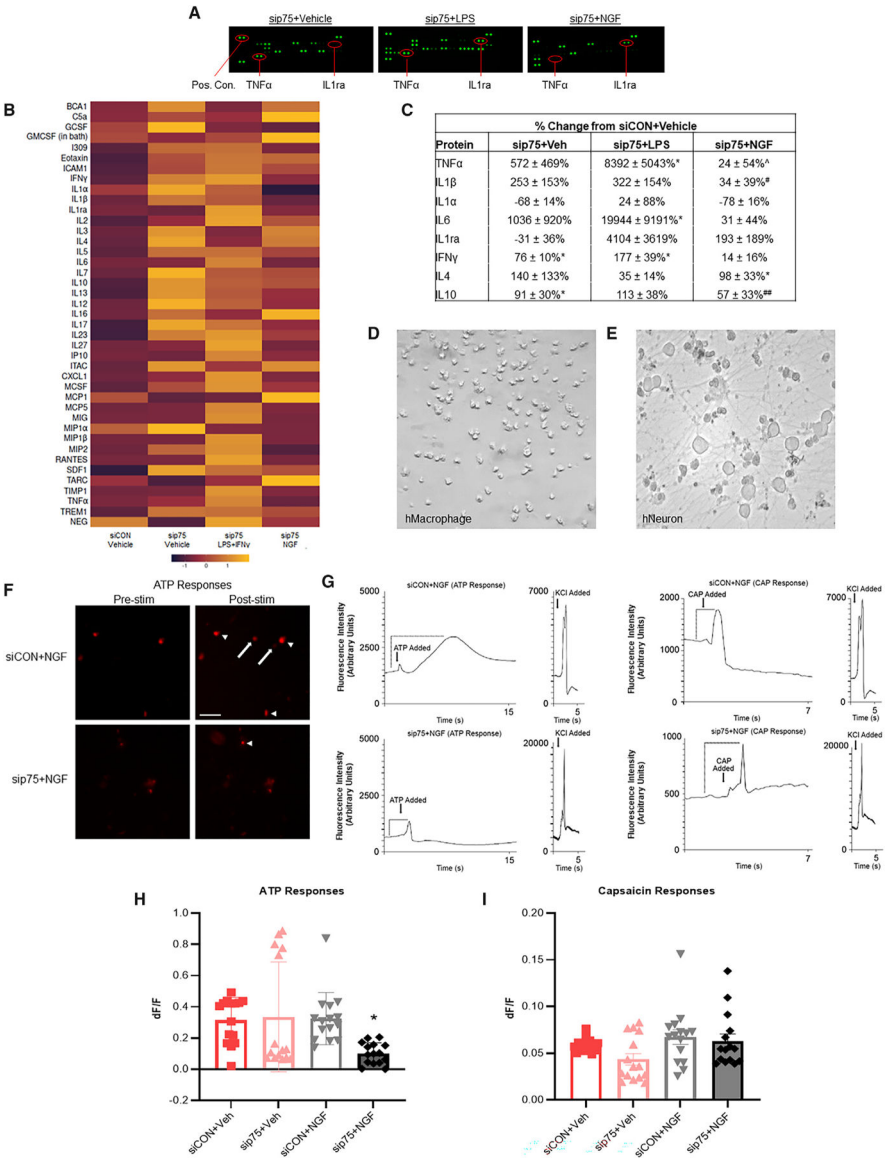

Figure 6. p75NTR expression in macrophages alters the inflammatory signature of macrophages and neuronal activity

(A) Example protein arrays of BMDM lysates with knockdown of p75NTR and stimulated with the indicated factors.

(B) Heatmap indicating protein expression detected across each stimulus; $n = 4$/group.

(C) Examples of significantly regulated proteins from the arrays (*$p < 0.05$ vs. siCON+Veh, ^$p < 0.05$ vs. sip75+LPS, #$p = 0.05$ vs. sip75+Veh, ##$p > 0.05$ vs. sip75+Veh; one-way ANOVA, Tukey's or ANOVA on ranks, Dunn's; $n = 4$/group).

(D–F) Representative images of iPSC-derived macrophages, sensory neurons, and Rhod-2 responses to ATP. Arrows, increased responses; arrowheads, new responses. Scale bar, 25 μm.

(G) Example calcium transients from iPSC-derived sensory neurons in response to ATP, capsaicin, or KCl. Arrows indicate when the ATP or capsaicin was added, and the brackets indicate the part of the trace that was analyzed to calculate responses. scale bar, 20 μM.

(H) Exposure of iPSC-derived sensory neurons to medium from macrophages with loss of p75NTR treated with NGF caused decreased responsiveness of neurons to ATP (F = 4.257) (*$p < 0.04$ vs. all other conditions, one-way ANOVA with Tukey's post hoc, $n = 15$ cells per group).

(I) No changes in capsaicin responses (F = 2.702) were observed (one way ANOVA). Mean ± SEM or percent change from controls with variance.

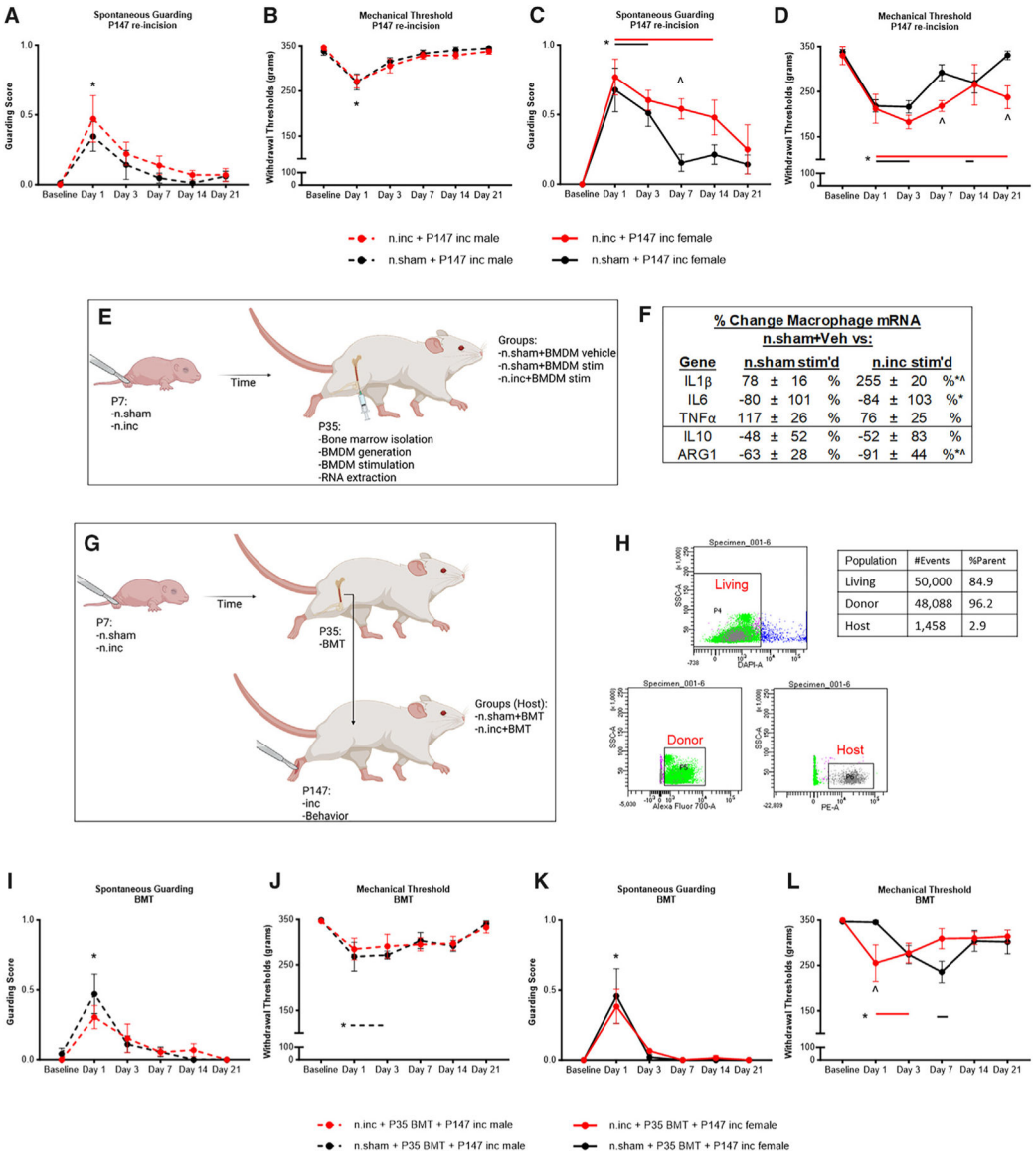

Figure 7. BMT from neonatal incised animals transfers a "pain memory" to naive animals

(A and C) There is a main effect of group ($F = 6.96$) and day ($F = 27.20$) for guarding, with post hoc analysis revealing that n.inc+P147 inc females guard through day 14 (*$p < 0.05$ vs. BL) and significantly more than n.sham +P147 females at day 7 ($^{\wedge}p = 0.02$). n.sham+P147 females guard through day 3 (*$p < 0.001$ vs. BL), while both male groups only guard at day 1 (*$p < 0.05$ vs. BL). Two-way RM ANOVA, Tukey's.

(B and D) For muscle squeezing, there is an interaction effect ($F = 3.50$). n.inc+P147 inc females have significantly reduced thresholds from BL for 3 weeks (*$p < 0.05$ vs. BL) and are significantly more hypersensitive than n.sham+P147 inc females at days 7 and 21 ($^{\wedge}p <$ 01 vs. n.sham+P147 inc female). n.sham+P147 inc females have reduced thresholds at days 1, 3, and 14, while males from both groups are hypersensitive at day 1 only (*$p < 0.05$ vs. BL). Two-way RM ANOVA, Tukey's, $n = 11–13$/injury condition, 4–7/sex in condition.

(E) Schematic of the timeline for neonatal nociceptive priming experiments separating injury by 140 days.
(F) mRNA changes from BMDMs after stimulation with LPS+IFNγ (*$p < 0.05$ vs. n.sham no stimulation controls, ^$p < 0.05$ vs. n.sham with stimulation [stim'd], n = 3–8/group, two-way ANOVA, Tukey's).
(G) Schematic of the BMT experiments.
(H) Representative cell sorting of living cells, 45.1+ host remaining cells, and 45.2+ transferred cells.
(I and K) After BMT, there is a main effect of day (F = 22.90). Animals display no guarding behaviors prior to incision. Following an incision, both n.sham and n.inc groups from both sexes guarded for 1 day only ($p < 0.01$ vs. BL, two-way RM ANOVA, Tukey's).
(J and L) For muscle squeezing, n.inc+P35 BMT+P147 inc females are hypersensitive to BL at days 1 and 3 (*$p < 0.05$ vs. BL) and have significantly lower thresholds than controls at day 1 (^$p = 0.013$ vs. n.sham+P35 BMT+P147 inc female). n.sham+P35 BMT+P147 inc females do not begin to display sensitivity until day 7 (*$p = 0.001$ vs. BL). n.sham+P35 BMT+P147 inc males have reduced thresholds from BL at days 1 and 3 (*$p < 0.05$ vs. BL). Two-way RM ANOVA, Tukey's, $n = 10–11$/injury condition, 4–6/sex in condition. Colored horizontal lines indicate the duration of significance compared to BL for each group. Mean ± SEM.

KEY RESOURCES TABLE

REAGENT or RESOURCE	SOURCE	IDENTIFIER
Antibodies		
WGA	Invitrogen	W32466
Dystrophin	Abcam	Ab15277; RRID:AB_301813
P75NTR	Cell Signaling	82385
F4/80	Abcam	Ab6640; RRID:AB_1140040
Chemicals, peptides, and recombinant proteins		
AP20187 (AP; B/B Homodimerizer)	Takara	635058
Evan's Blue Dye	Sigma	E2129–10
Critical commercial assays		
Proteome profiler	R&D Systems	ARY006
RNeasy Mini Kits	Qiagen	74104
Deposited data		
ATAC-seq and RNA-seq	This paper	NCBI: GSE224209
Other Data	This paper	Mendeley Data: https://data.mendeley.com/datasets/xbm7kxddjt/draft?a=f13b0ef2-3721-4283-97b2-41d8e5cd2d66.
Experimental models: Cell lines		
Human iPSC $CD14^+$ monocytes	ATCC	DYS0100
Human iPSC Sensory neuron progenitors	AXOL	Ax0555
Experimental models: Organisms/strains		
C57/Bl6 (CD45.2+)	Jax	000664
B6.SJL/BoyJ (CD45.1+)	In house	N/A
MaFIA	Jax	005070
LysM-Cre	Jax	004781
B6.Cg-Gt(ROSA)26Sortm14(CAG-tdTomato)Hze/J	Jax	007914
LysM-CreERT2	Jax	031674
p75NTRfl/fl	Donated	N/A
Oligonucleotides		
TNFα FWD	IDT	CCTATGTCTCAGCCTCTTCT
TNFα REV	IDT	GGGAACTTCTCATCCCTTTG
IL1β FWD	IDT	TACAAGGAGAACCAAGCAAC
IL1β REV	IDT	GGTGTGCCGTCTTTCATTA
IL6 FWD	IDT	ACTGATGCTGGTGACAAC
IL6 REV	IDT	CCGACTTGTGAAGTGGTATAG
IL10 FWD	IDT	CAGCCGGGAAGACAATAAC

REAGENT or RESOURCE	SOURCE	IDENTIFIER
IL10 REV	IDT	CAGCTGGTCCTTTGTTTGA
ARG1 FWD	IDT	TTGGGTGGATGCTCACACTG
ARG1 REV	IDT	TTGCCCATGCAGATTCCC
Other		
siRNA against p75NTR – Human	Origene	SR321107
siRNA against p75NTR – Mouse	Origene	SR414146